JMEPEG (2022) 31:1707–1727
https://doi.org/10.1007/s11665-021-06355-2

1059-9495/$19.00

Corrosion, Corrosion Fatigue, and Protection of Magnesium Alloys: Mechanisms, Measurements, and Mitigation

Temitope Olumide Olugbade, Babatunde Olamide Omiyale, and Oluwole Timothy Ojo

Submitted: 28 March 2021 / Revised: 23 September 2021 / Accepted: 27 September 2021 / Published online: 29 October 2021

Magnesium (Mg) alloys are non-toxic, biodegradable, and biocompatible special metallic biomaterials for biomedical applications, but less corrosion-resistant in physiological and chloride-containing environments. This often limits their use as potential biomedical implants due to loss of their mechanical integrity. This can be addressed by adopting several approaches such as surface modifications and coatings as well as pre-treatments including anodization, microarc oxidation, and electrodeposition. To further provide insights into better ways to improve the corrosion resistance of Mg alloys in saline and physiological environments, the present work provides a comprehensive overview of the electrochemical properties of Mg alloys as a biodegradable material. More importantly, the corrosion and corrosion fatigue mechanisms in surface-modified Mg alloys are explicitly reviewed. The significant influence of alloying on the corrosion resistance behaviors of biodegradable Mg alloys is also reviewed and discussed explicitly. The different methods of measuring the corrosion rates of Mg and its alloys are reviewed and summarized. As potential implant materials, the recent progress and developments on Mg alloys in the biomedical fields and their resulting corrosion properties are discussed and the research trends for future works are highlighted.

Keywords corrosion, corrosion fatigue, crack, implant, Mg alloy, surface treatment

Abbreviations

Mg	Magnesium
SCE	Saturated calomel electrode
OCP	Open-circuit potential
CFS	Corrosion fatigue strength
CAC	Corrosion-assisted cracking
i_{corr}	Corrosion current density
E_{corr}	Corrosion potential
i-SBF	Ionized simulated body fluid
r-SBF	Revised simulated body fluid
PBS	Phosphate-buffered saline
SBF	Simulated body fluid
m-SBF	Modified simulated body fluid
DMEM	Dulbecco's phosphate dehydrate
c-SBF	Conventional simulated body fluid
SCC	Stress corrosion cracking
EIS	Electrochemical impedance spectroscopy
NaCl	Sodium chloride
DIW	Deionized water
ATW	Artificial tap water
SNC	Surface nanocrystallization
HE	Hydrogen embrittlement
HA	Hydroxyapatite
PSC	Perovskite solar cells
Pt	Platinum
M-Mg	Milled pure magnesium

1. Introduction

1.1 Corrosion and Fatigue Properties of Mg Alloys

Metallic implant materials such as cobalt-based alloys, stainless steels, titanium alloys, and magnesium (Mg) alloys are often used as temporary implants due to their exceptional properties including high strength and biodegradability (Ref 1-3). They are primarily used as a temporary internal support for bones, tissues, etc. (Ref 4, 5) and are usually removed from the body through surgery when their purpose are fulfilled. Belonging to the family of metallic biomaterials, Mg alloys are the promising candidates in orthopedics and biomedical fields due to their biocompatibility and biodegradability (Ref 6-9), and easy dissolution in the body (Ref 10-13). They are also vital in human metabolism process; the degradation products of Mg are thus not toxic or harmful to the body.

However, the poor corrosion resistance of Mg alloys in saline and physiological environments (Ref 14-18) remain a constant threat for Mg alloys as potential orthopedic implants (Ref 2, 4, 11). The Mg alloys corrode rapidly in chloride-containing environments which limits their use as implants due to loss of their mechanical integrity and stability before actualizing their purpose (Ref 5, 14, 15, 18). The chloride-containing environments couple with the cyclic loading usually experienced by the Mg alloy implants can result in corrosion-assisted cracking (CAC). The poor corrosion resistance of Mg alloys in aqueous environments may be attributed to their high chemical and electrochemical reactivity.

Temitope Olumide Olugbade, Babatunde Olamide Omiyale, and **Oluwole Timothy Ojo**, Department of Industrial and Production Engineering, Federal University of Technology, P.M.B. 704, Akure, Ondo State, Nigeria. Contact e-mail: tkolugbade@futa.edu.ng.

Corrosion-assisted cracking often leads to sudden premature failure of materials under the combined actions of mechanical loading and corrosion reaction (corrosion fatigue), and the failure mode largely depends on the nature of loading (Ref 25). While the corrosion fatigue is usually induced by cyclic loading (Ref 19) leading to catastrophic failure of biomedical implants (Ref 20-22), the stress corrosion cracking (SCC) often results from tensile loading (Ref 23-27). Interestingly, the corrosion fatigue failure (Ref 28) of materials can occur even at low stress amplitude. Stress corrosion cracking of Mg alloys has been a subject of investigation over the years in different environments (Ref 29, 30) with dissolution-assisted cracking and hydrogen embrittlement (HE) as the main two mechanisms.

Apart from exhibiting a good corrosion fatigue strength, an improvement in the general corrosion properties in corrosive environments alone (absence of cyclic loading) has been achieved over the years for alloys (Mg, Ti, etc.,) and metallic materials including stainless steels (Ref 31-34). Several methods adopted in the past to enhance the general corrosion properties and reduce the degradation rate include coatings/electrodepositions (Ref 35-38), laser cladding and thermal spraying (Ref 39), machining/molding (Ref 40), alloying, and surface nanocrystallization (SNC) (Ref 41-47).

Under the combined actions of cyclic loading and corrosion reaction, the corrosion fatigue strength (CFS) of Mg alloys is an important property till date and ways to significantly enhance it remain a major subject of investigation for many corrosion experts and material scientists. To give new insight to the readers, the present review therefore surveys the existing works on the fatigue and corrosion fatigue mechanisms of Mg alloys, especially when subjected to surface treatments.

1.2 Contribution of the Present Study

The present review contributes to knowledge in four different ways.

(1) The different methods of determining the corrosion rates of Mg and its alloys are reviewed and summarized including the polarization method via Tafel extrapolation technique, weight loss method, hydrogen evolution method, rate of Mg^{2+} leaving the metal surface, electrochemical impedance spectroscopy (EIS) analysis, and immersion test.
(2) The corrosion and corrosion fatigue mechanisms of Mg alloys are ascertained with the view of identifying the influencing factors such as rate of exposure to the environment, operating conditions, and temperature. Hence, producing an ultra-high and strong Mg alloy with excellent corrosion and wear resistance is one of the turning points of the present research. This is necessary to obtain a biocompatible special metallic biomaterial which can withstand the corrosive environments over time.
(3) To a large extent, alloying elements have a significant effect on the corrosion resistance behavior of biodegradable Mg alloys. The extent of alloying influence on the degradation rate of Mg alloy as well as the mix ratios for the alloying elements is worthy of further investigation and hence one of the areas of the present work.
(4) As possible solutions to the poor corrosion resistance of Mg alloys, especially in physiological environments, the several methods of enhancing the corrosion properties of Mg alloys including alloying, surface treatment, and coating processes are provided, which will be of great use to many material scientists and corrosion experts.

2. Corrosion Rate Evaluation Methods

Generally speaking, the corrosion rates of Mg alloys can be evaluated using different methods including (a) polarization method via Tafel extrapolation technique (P_i in mm/y), (b) weight loss method (P_W in mm/y), (c) hydrogen evolution method (P_H), (d) rate of Mg^{2+} leaving the metal surface, (e) electrochemical impedance spectroscopy (EIS) analysis (P_{EIS}), and (f) immersion test (Ref 5, 7, 16, 17).

By obtaining the value of the corrosion current density (i_{corr}) from the cathodic branch of polarization curve via Tafel extrapolation method, the evaluation of the corrosion rates of Mg and its alloys via polarization technique (P_i in mm/y) are often carried out using the following relationship (the i_{corr} is related to the average penetration rate and the constant is a function of the pH and concentration of the solution) (Ref 5, 17),

$$P_i = 22.85 \times i_{corr}\left((i_{corr}) \text{ in } \text{mA/cm}^2\right) \quad \text{(Eq 1)}$$

Provided the immersion time (t in day), surface area (A in cm^2), sample weight before immersion (W_2 in g), and sample weight after immersion (W_1 in g) are known, the corrosion rates of Mg alloys can be evaluated using weight loss method (P_W in mm/y) with the relationship below (the constant is a function of the mol of the Mg metal and the corrosion area for each mol of Mg metal) (Ref 7, 17),

$$P_W = 2.1 \times \frac{W_1 - W_2}{At} \quad \text{(Eq 2)}$$

Meanwhile, using the hydrogen evolution method (P_H in mm/y) and provided the immersion time (t in day), surface area (A in cm^2), and the volume of the evolved hydrogen (V_H) are given, the corrosion rates of Mg alloys can be easily determined using the following relationship (Ref 5, 16),

$$P_H = \frac{2.088 \times V_H}{At} \quad \text{(Eq 3)}$$

Furthermore, using the immersion test (P_{im}) method, the corrosion rate of Mg alloys can be evaluated via the following relationship (Ref 7),

$$P_{im} = \frac{(K \times W)}{(A \times T \times D)}(4) \quad \text{(Eq 4)}$$

where D is the material density (g/cm^3), T is the time of exposure (h), A is the sample surface area, W is the mass loss (g), and K is a constant (87,600).

It is important to note that using only one method to evaluate the corrosion rate of Mg alloys is not enough and reliable. To ensure accuracy, reliability, and reproducibility, two or more measurement methods should be adopted in evaluating the corrosion rate of Mg alloy. For instance, hydrogen evolution method and weight loss methods can be adopted to cross-check the corrosion rates of Mg alloy determined using polarization and electrochemical methods. Generally speaking, the unit of mm/y is applicable for the determination of corrosion rate evaluation on long-term basis. Since heterogeneous corrosion is

often applicable for Mg alloys, short-term tests such as polarization and immersion methods are not suitable for the evaluation of the long-term corrosion rate.

Hence, it is advisable to use different methods in evaluating the corrosion rates of Mg alloy instead of the independent measurement. By this, the measurement methods can complement each other in that the shortcomings experienced with one method can be overcome with other measurement methods. Furthermore, for uniformity's sake, the corrosion measurement methods should be converted and compared using the same units.

Some measurement issues related to the corrosion rate determination has been identified. Using the polarization method via Tafel extrapolation technique, the curvature of cathodic curves denotes an increase in polarization results and hence an increase in resistance (Ref 7, 43, 44). In addition, measurements at short times may not typically represent the corrosion mechanism in a steady state; hence, the most appropriate immersion time should be given much consideration. Furthermore, a condition known as the negative difference effect is also common with the polarization method. On the other hand, some challenges are related to hydrogen evolution method as a means of evaluating the corrosion rate of Mg alloys. For instance, there is a need to put into consideration the dissolution of some hydrogen in the Mg sample in solutions such as Nor's solution as well as the aftermaths. Furthermore, careful consideration should be given to the mode of collection of the evolved hydrogen so as to prevent the introduction of other gases such as carbon dioxide into the solution. As regards the weight loss method, there is a possibility of removing the Mg metal while removing the corrosion products after exposure to the corrosive environment. In addition, a steady-state condition may not be reached due to the appreciable error that might occur as a result of the difference in mass before and after immersion. In this case, hydrogen evolution method may be the best option for the corrosion test evaluation because of its long-term effect and less impurities obtained during the process. In addition, using the hydrogen method to evaluate the corrosion rate of Mg alloys, unlike the conventional weight loss and electrochemical methods, apart from the provision of the final corrosion information, errors are not likely to be introduced during the measurements of the corrosion rate though the weight loss measurement because it is simple and easy to carry out. However, hydrogen evolution method may be hard to achieve during the corrosion fatigue measurements due to the possible dissolution of part of hydrogen into the Mg matrix.

3. Corrosion Fatigue of Mg Alloys

The fatigue crack initiation is rampant at the stress concentration sites which is caused as a result of some defects during the manufacturing process including inclusions and pores, as well as surface defects and depressions during casting. Depending on the stress intensity factor value (Ref 58), the environments often influence the corrosion fatigue behavior. The corrosion fatigue behavior of Mg alloys in different corrosive environments and applications at different temperatures are summarized in Table 1 (Ref 48-62). The corrosive environments range from sodium chloride (NaCl), simulated body fluid (SBF), and modified simulated body fluid (m-SBF). For instance, in gear oil, the addition of epoxy coating enhances the fatigue limit of Mg-3Al-1Zn alloy (Ref 50) making it a promising candidate for aerospace and automotive applications. This is because the epoxy coating prevents the direct contact between the Mg alloy and the corrosion environment, hence reducing the corrosion rate, though the mechanical property of the coating tends to reduce too leading to fatigue crack initiation. However, using gear oil as the corrosive medium may result in flaking off of the epoxy coating on the Mg alloy. In sodium sulfate solution, a similar improvement in the corrosion fatigue limit is observed for AZ31 Mg alloy coated with epoxy (Ref 59). The enhancement in the fatigue limit as well as the mechanism behind the fatigue crack initiation may be attributed to the strain matching action between the Mg alloy and the pore-free epoxy coating making the alloy less prone to corrosion. The case is different for Mg-4Al-2Ba-2Ca alloy in chloride-containing environment where the fatigue limit decreases with an increase in NaCl concentration. The decrease in the fatigue limit and corrosion resistance may be linked to the measurement change in open-circuit potential and plastic strain (Ref 54). Ensuring stable connection and stability between the Mg alloy and the chloride solution may address the issue of decreased fatigue limit and corrosion resistance, hence maintaining its lightweight applications. However, in NaCl solution, a decrease in corrosion fatigue resistance is observed for Mg alloy due to the increase in thickness of the anodized coating. In short, we can say that the roughness at the painting/anodized interface is the decisive factor for determining the corrosion fatigue strength (Ref 60). In other words, painting and coating as forms of surface treatments can protect the Mg alloy from the corrosive environment attacks (Ref 51).

The ion concentrations and compositions of the solutions during corrosion fatigue of Mg alloys are also very important and need to be properly considered. As a matter of fact, ringers (Ref 63), ionized simulated body fluid (i-SBF) (Ref 64), modified simulated body fluid (m-SBF) (Ref 65), or revised simulated body fluid (r-SBF) (Ref 66, 67) among others (Ref 68-71) are composed of Cl^-, buffer, SO_4^{2-}(mmol L^{-1}), HPO_4^{2-} (mmol L^{-1}), HCO_3^- (mmol L^{-1}), Mg^{2+} (mmol L^{-1}), Ca^{2+} (mmol L^{-1}), Na^+, K^+ (mmol L^{-1}).

Through corrosion potential responses, the cracking process can be controlled; hence, the corrosion fatigue strength is directly linked with the corrosion rates of materials (Ref 48). It is important to note that the level of humidity of the environment can influence the corrosion fatigue strength of Mg alloy. For instance, the fatigue strength of AM60 alloy reduces with increasing level of humidity (Ref 49). This may be as a result of the presence of corrosion-induced defects on the material surface. Meanwhile, the fatigue strength of AZ61 alloy reduces greatly in sodium and calcium chlorides environments as well as high-humidity environment. The reason for this is not farfetched; due to the low Ph value and high level of Cl^-, the chloride-containing environment facilitates the formation of pit and growth as compared with the calcium chloride environment (Ref 52). If not properly monitored, the pit growth can escalate until a critical size for crack nucleation is reached. This is another reason behind the reduction in fatigue strength experienced by AZ61 alloy.

Studying the fatigue strengths of various Mg alloy, several factors including coatings, surface finishing, plastic deformation, heat treatments, and microstructure, cyclic loading, and sometimes wear (Ref 53, 58) could influence the corrosion fatigue mechanism. Figure 1 summarizes the fatigue strengths

Table 1 Corrosion fatigue behavior of Mg alloys in different corrosive environments and applications

S/N	Materials	Corrosive environments	Applications	References
1	Mg alloy DieMag422	0, 0.001, 0.01, and 0.1 mol L^{-1} NaCl	Automotive	48
2	Mg alloy AE42	0, 0.1, 1mol L^{-1} NaCl	Automotive	48
3	AM60 Mg alloy	(i) Relative humidity 55% RH (ii) Relative humidity 80% RH (iii) 5% NaCl	Automotive construction	49
4	Mg-3Al-1Zn alloy	Gear oil	Aerospace Automotive	50
5	AZ61 Mg alloy	(i) Relative humidity 55% RH (ii) Relative humidity 80% RH (iii) 5% NaCl	Lightweight engineering applications	51
6	AZ61 Mg alloy	(i) Relative humidity 55% RH (ii) Relative humidity 80% RH (iii) 5% NaCl	Structural materials in automobile	52
7	AZ91D Mg alloy	Simulated body fluid (SBF) at 37 °C	Biodegradable biomaterials	53
8	WE43 Mg alloy	SBF at 37 °C	Biodegradable biomaterials	53
9	Mg alloy Mg-4Al-2Ba-2Ca	(i) Double distilled water (ii) 0.01 and 0.1 mol L^{-1} NaCl	Lightweight applications	54
10	Mg alloys	Simulated body fluid (SBF)	Bioimplants	55
11	Mg alloy	Modified simulated body fluid (m-SBF)	Biodegradable implants	56
12	Mg alloy	(i) Air (ii) Hanks' solution	Bioimplants	57
13	Biomedical metallic alloys	3.5 wt.% NaCl solution	Metallic implants	58
14	AZ31 Mg alloy	3.5 wt.% Na_2SO_4 solution	(i) Aerospace (ii) Electronic communications	59
15	Mg alloy	3% NaCl solution	Structural materials	60
16	MgZn1Ca0.3 (ZX10)	(i) Air (ii) m-SBF	Biodegradable implants	61
17	Mg alloy	(i) Air (ii) 3% NaCl	Structural materials	62

of various Mg alloy with a view to studying the trend of fatigue strength improvement under fatigue loading conditions (Ref 48-51, 54-57, 59, 72-76). For instance, under the same environment (low humidity), with the fatigue strength of 140 MPa for coated AZ61 (Ref 51), 135 MPa for bulk AZ61 (Ref 51), 100 MPa for shot-blasted AM60 (Ref 49), and 80 MPa for as-cast AM60, the fatigue strength increases due to the extent of heat treatment and surface finishing. Similar trend was observed under high-humidity environment for as-cast AM60, shot-blasted AM60, bulk AZ61, and coated AZ61 with increasing fatigue strengths of 53 MPa (Ref 49), 90 MPa (Ref 49), 105 MPa (Ref 51), and 140 MPa (Ref 51), respectively. This tendency of increasing fatigue strength across Mg alloys is illustrated in Fig. 1. It can be deduced from the trend and pattern that the fatigue strength increases with Mg alloy materials depending on the type and nature of material treatment. This indicates that the extent of surface treatment, plastic deformation, and surface finishing has a great influence on the fatigue strengths of Mg alloys.

In air, the AZ91D alloy possesses a higher corrosion fatigue strength as compared with simulated body fluid (SBF). In SBF, the corrosion pits are responsible for the fatigue crack initiation while micropores are the main reasons behind the fatigue crack initiation in air (Ref 53). Likewise in Hanks' solution, cracks are initiated from corrosion pits and from inclusions and defects in air as regards AZ91 Mg alloy (Ref 57) and Mg-Zn-Y-Nd alloy (Ref 74). Furthermore, hydrogen embrittlement and stress corrosion can also result in fatigue crack initiation in SBF. Cracks may also initiate from depressions along the interface between the coated layer and Mg alloy and from depression on the sample surface (Ref 62). The implication of this is that the fatigue life can be greatly enhanced if the surface defects and depressions imported during the manufacturing process are eliminated. Mg alloy ZX50 may find a great application as biodegradable implants due to its excellent corrosion fatigue resistance. The exceptional corrosion fatigue resistance may be linked to the non-appearance of cathodic intermetallic phases and strengthening of the grain boundary (Ref 61). The fatigue limits of selected Mg alloys in different media are summarized in Table 2 while Table 3 shows the mechanical integrity of selected pre-corroded Mg alloys at room temperature.

In simulated physiological environments, the localized corrosion and pitting corrosion are the principal mechanisms of Mg alloys. During the corrosion process, the corrosion products include the H_2 gas, large amount of OH-, dissolved Mg ions, and the corroded surface. To further enhance the corrosion fatigue behavior and the mechanical properties in biological medium, Mg composites consisting of matrix and reinforcement obtained from nutritional elements can be developed. The enhanced properties exhibited by the composite can be attributed to the self-healing property of the reinforcement. Furthermore, forming composites from bioactive or bioinert ceramics results in mechanical strength and biocompatibility. In addition, incorporating the use of ternary alloy systems including Mg/Cu/Au and Mg/Pb/Bi (even though brittle) and binary systems including platinum, silver, bismuth, cadmium, and aluminum may also improve the corrosion resistance properties of Mg alloys. Magnalium which is

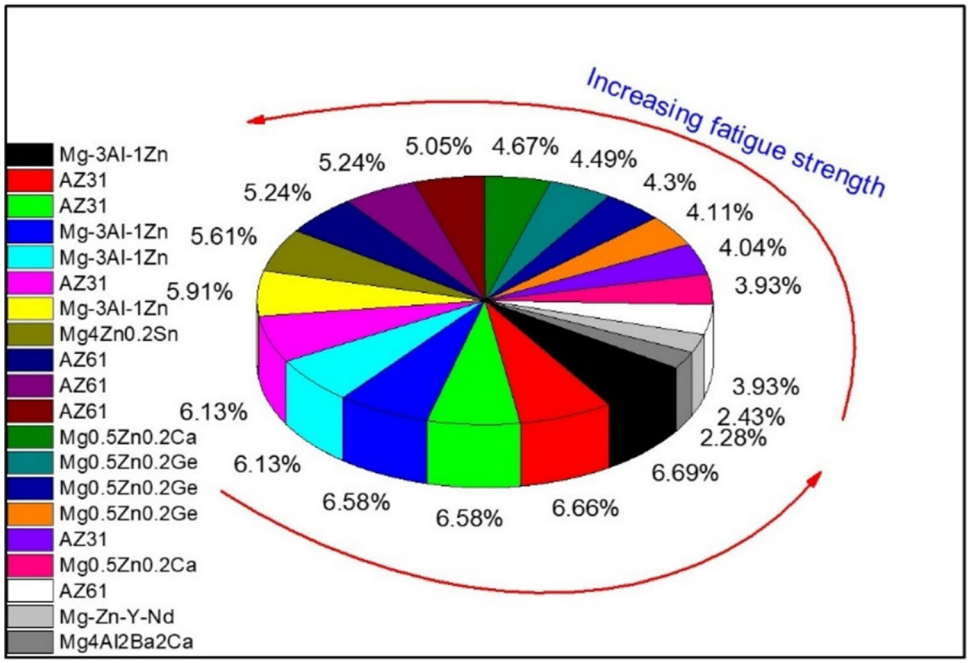

Fig. 1. Summary of the fatigue strengths of various Mg alloy with a view to studying the trend of fatigue strength improvement under fatigue loading conditions (data compiled from (Ref 48-51, 54-57, 59, 72-76))

obtained from the combination of few amounts of magnesium and aluminum is also a promising way of improving the overall corrosion properties of Mg. In studying the corrosion process of Mg in vivo, it is important to consider the content of the local water of the surrounding tissue Mg and the content of the local H_2 carbonic acid.

From the authors' point of view, the proneness of Mg alloy to corrosion limits its application in automobile and other manufacturing industries. To a large extent, the solution's acidity and corrosion medium directly influence the corrosion fatigue life of Mg alloy. For instance, the fatigue life of Mg alloy tends to be higher in air than when subjected to chloride-containing environment or immersed in simulated body fluid (SBF). Hence, care should be taken in aggressive environments to prevents corrosion fatigue damage and premature failures. The corrosion resistance properties of Mg can further be strengthened by adopting the surface coating method. Surface treatment tends to create a thick dense surface layer on the material surface, hence protecting the material from external attack, especially when exposed to aggressive environments. It is important to know that the localized corrosion and corrosive environments can influence the mechanical integrity of Mg alloys. As indicated in Table 3, the $Mg_{0.5}Zn_{0.2}Ca$ alloy exhibited a lower yield and ultimate tensile strengths of 111 and 217 MPa, respectively, compared to $Mg_{0.5}Zn_{0.2}Ge$ alloy with higher mechanical integrity (yield strength of 166 MPa and ultimate tensile strength of 241 MPa) (Ref 73). Under the same conditions, the mechanical integrity in terms of the yield and ultimate tensile strengths for $Mg_{0.5}Zn_{0.2}Ca$ alloy is lower than that of $Mg_{0.5}Zn_{0.2}Ge$ alloy under severe corrosive environments. The decrease in mechanical integrity can be linked to the appearance of the localized corrosion as well as the reduction in areas of the real loading during service lives. To sum it up, without the proper protection methods via coating or nanocrystallization, the exposure of Mg alloy to aggressive environments will result in poor corrosion fatigue strength and rapid deterioration in mechanical integrity in terms of tensile properties.

4. Alloying Element–Corrosion Behavior Relationship

Several efforts have been explored in the past to significantly enhance the corrosion resistance of Mg alloys since they remain a potential candidate for many biomedical, automotive, and aerospace applications. Presently, alloying, surface treatment, and coating processes are receiving wide attentions as possible solutions to the poor corrosion resistance of Mg alloys, especially in physiological environments. Due to its texture weakening effect and grain refinement, alloying elements like Nd (Ref 75) can effectively enhance the ductility of Mg. In addition, the addition of other alloying elements such as Sn, Sb, Si, Ca (Ref 75), La, Ce, Y, and As have been experimented to effectively quantify the extent the corrosion resistance of Mg alloys can be enhanced. By making the alloy nobler and generating a surface protecting layer, Zn can improve the corrosion potential of Mg as well enhance the mechanical property through solution hardening mechanism. Al immensely contributes to corrosion resistance enhancement as regards the distribution and intermetallic content while an improvement in the corrosion resistance experienced with the addition of Sn-Mg alloys can be attributed to the presence of phases in the alloy.

To a large extent, the presence of certain alloying elements including Sn, Sr, Nd, Y, Ca, and Zn (Ref 76-82) can enhance the corrosion resistance behavior (Ref 82, 83) as well as the mechanical properties (Ref 78, 81) of biodegradable Mg alloys. An improvement in mechanical properties of Mg alloys can also be achieved through the addition of reinforced particles including tricalcium phosphate (Ref 84), calcium polyphos-

Table 2. Fatigue limits of selected Mg alloys in different media

S/N	Mg alloys	Medium	Corrosion rates, mg a^{-1} cm^{-2}	Fatigue strength, MPa	References
1	DieMag422	0.1 mol NaCl	$2.4 \cdot 10^4$	…	48
2	AE42	0.1 mol NaCl	$1.3 \cdot 10^4$	…	48
3	AM60 (as-cast)	(i) Low humidity (55% RH)		80	49
		(ii) High humidity (80% RH)	…	53	
		(iii) 5% NaCl	…	20	
4	AM60 (shot-blasted)	(i) Low humidity (55% RH)	…	100	49
		(ii) High humidity (80% RH)	…	90	
		(iii) 5% NaCl		50	
5	Mg-3Al-1Zn (uncoated)	(i) Air	…	164	50
		(ii) Gear oil	…	158	
6	Mg-3Al-1Zn (coated)	(i) Air	…	176	50
		(ii) Gear oil	…	179	
7	AZ61 (bulk)	(i) Low humidity	…	135	51
		(ii) High humidity	…	105	
		(iii) NaCl	…	20	
8	AZ61 (coated)	(i) Low humidity	…	140	51
		(ii) High humidity	…	140	
		(iii) NaCl	…	120	
9	Mg-4Al-2Ba-2Ca	(i) 0 mol NaCl	100	61	54
		(ii) 0.01 mol NaCl	3100	58	
		(i) 0.1 mol NaCl	7200	54	
10	AZ31 (uncoated)	(i) Air	…	164	59
		(ii) 3.5% Na_2SO_4	…	108	
11	AZ31 (coated)	(i) Air	…	176	59
		(ii) 3.5% Na_2SO_4	…	178	
12	Mg4Zn0.2Sn	(i) Air		150	72
		(ii) 0.5 wt.% NaCl-DIW		120	
13	Mg0.5Zn0.2Ca	(i) Air		125	73
		(ii) 0.5 wt.% NaCl-ATW		115	
		(iii) 0.5 wt.% NaCl-DIW		105	
14	Mg0.5Zn0.2Ge	(i) Air		120	73
		(ii) 0.5 wt.% NaCl-ATW		115	
		(iii) 0.5 wt.% NaCl-DIW		110	
15	Mg-Zn-Y-Nd	Air		65	74, 75

Table 3. Mechanical integrity of selected pre-corroded Mg alloys at room temperature

S/N	Mg alloys	Tensile strength, MPa	Yield strength, MPa	Elongation, %	References
1	$Mg_4Zn_{0.2}Sn$	216	149	7	72
2	AE42	128	21	6	48
3	AZ31	220	148	7	75
4	$Mg_{0.5}Zn_{0.2}Ge$	241	166	10	73
5	AZ61	318	185	18	51, 52
6	Mg-0.47Ca	180	90	15	75
7	Mg-2Nd	210	83	18	75
8	Mg-Zn-Y-Nd	229	159	27	74
9	AZ31	275	200	11	60, 62
10	AZ91D	180	105	2	56, 57
11	Die-cast AZ91	71	171	4	53
12	Mg-3Al-1Zn	22	19	2	50, 58
13	AM60	224	103	9	49
14	$Mg_{0.5}Zn_{0.2}Ca$	217	111	18	73
15	DieMag422	107	27	1	48

phate (Ref 85), hydroxyapatite (Ref 77, 86), and calcium phosphate-based ceramics (Ref 86-88). Promising Mg alloys designed for biomedical applications (Mg-Zr, Mg-Sr, Mg-Si, Mg-Zn, Mg-Ca, Mg-Sn, Mg-Mn, Mg-Ag, etc.) (Ref 89-92) are presently receiving wide attention due to their non-toxic behavior in physiological environments.

In biodegradable Mg alloys, alloying elements which can be nutrient-based (Zn, Sn, Mn, Ca, etc.,), allergic (V, Ni, Cu, Cr,

Al, etc.,), or toxic (Cd, Be, Ba, etc.) (Ref 93-95) play significant roles like an improvement in corrosion and mechanical properties, strengthening of solid solution, and enhancement in grain refinement (Ref 96, 97). For instance, Zn and Mn can improve the yield stress and corrosion resistance, respectively, and the corrosion resistance and compressive strength can be greatly improved with the addition of Sn (Ref 78), whereas the grain refinement as well as corrosion resistance can be enhanced with the addition of Ca (Ref 75). The improved corrosion resistance associated with the addition of Sn can be attributed to the high rate of hydrogen evolution which greatly promote passivation behavior (Ref 72, 78, 95).

The relationship between alloying elements and electrochemical properties of Mg Alloys is illustrated in Fig. 2 (Ref 75-82, 93-95), showing the influence of alloying elements on the cathodic and anodic reactions, and the resultant effects on the corrosion resistance behavior. The graph (Fig. 2) is constructed from the polarization data obtained from the literature and the significance level of the alloying elements is interpreted along the arrows in up, down, left, and right directions. Due to the suppression of cathodic kinetics, the addition of As element in minute quantity reduces the corrosion rate of Mg alloy. Due to their insolubility, Cu, Ni, and Fe are the most common impurities in Mg alloys leading to accelerated cathodic kinetics. A similar increase in cathodic kinetics can be observed with Au, Ag, and Zr elements. Zr, Pb, and Sn improves the anodic reaction rate since they are nobler than Mg, whereas Ca and Li increases the anodic reaction rate since they are more electrochemically active than Mg. It can be deduced that the alloying elements such as Ce, La, Nd, Gd, Ga, Ti, and Si have minor effects on the anodic kinetics. A similar case can be said about Mn and Sc with minor effects on the cathodic kinetics of Mg alloy.

Alloying has been identified as one of the effective methods of enhancing the corrosion resistance of Mg alloys, and the influence of the independent alloying elements such as Ca, Zn and Al on the corrosion resistance behavior has been extensively discussed in the present paper. However, the

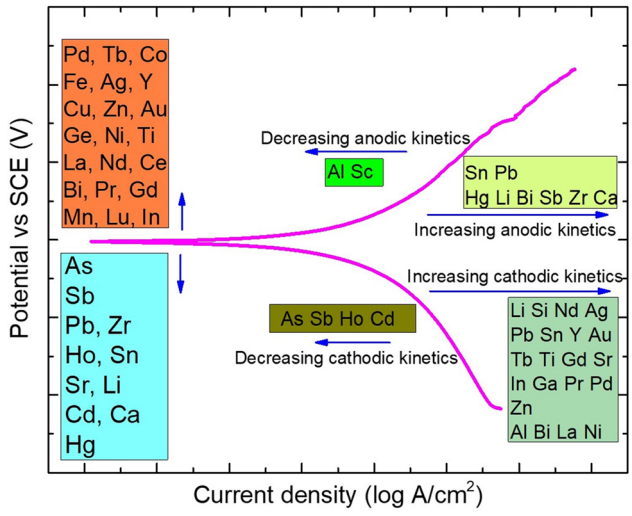

Fig. 2. Relationship between alloying elements and electrochemical properties of Mg Alloys showing the impacts of the alloying elements on the cathodic and anodic reactions and the resultant effects on the corrosion resistance behavior (data compiled from (Ref 75-82, 93-95))

combined effects of three or more alloying elements (Al-Sn-Zn, Ca-Zn-Al-Si, Sn, Sr-Nd-Y-Ca-Zn) on the corrosion resistance behavior of Mg alloys are yet to be fully explored and hence will serve as good subjects of investigations in future research on Mg alloys.

Mg alloys are often used as implants for replacing a broken or dislocated bone. One good thing about Mg implant is that once inserted in the human body, the properties are reliable in the sense that second surgeries are often prevented which is common to other materials. Despite their good mechanical and biodegradable properties, Mg alloys are less corrosion-resistant which put its good implant property under check because the corroded implant inside the body may lead to fatal and irredeemable damage. Hence, alloying plays a vital role in the corrosion enhancement of Mg alloys. With the presence of elements such as Cr, Ca, Al, Sr, which have a higher capacity of causing passivation than Mg, the corrosion resistance property of Mg can be greatly enhanced. This is made possible because the alloying elements tend to dominate the material surface. The corrosion properties are not only enhanced, but some alloying elements such as Ni and Cu also improve the overall mechanical properties. Hence, alloying elements can be referred to as corrosion resistance enhancer or booster. However, it is important to consider the bioproperties such as bioactivity, biodegradability, and biocompatibility in alloying of Mg alloys. For instance, NI and Cu are not adaptable to be used in bio-Mg alloys. In the field of biomaterials, alloying of Zn and Ca as well as rare elements such as Gd, Y, Pr, Nd, La, and Ce with Mg can fit perfectly when considering bioproperties of Mg alloys. In fact, Zn and Ca are probably the most biocompatible elements with Mg (Ref 15). Due to its beneficial effects including high thermodynamic stability, lack of toxicity, and improved corrosion resistance (Ref 4, 21, 53, 77), alloying of Y with Mg is now current practice as far as the biocompatibility of Mg alloys is concerned.

5. Surface-Treated Mg Alloys for Corrosion Protection

Surface treatment is one of the important methods of addressing the fast degradation rate and poor corrosion resistance issues of Mg alloys. This is often achieved by subjecting the Mg alloys to several surface treatments leading to the formation of protective layers on the surface, thereby reducing the rate of corrosion to the minimum. Generally speaking, anodization, electrodeposition, dip coating, microarc oxidation, etc. are the common methods of surface treatments (anticorrosion processing) for the corrosion protection of Mg alloys.

As reviewed in the schematics of surface-modified Mg alloys including the properties and applications (Fig. 3), Mg alloys are obviously non-toxic, biodegradable, and biocompatible (in terms of functionalization and stability) materials which are often used as biomedical implants. As summarized in Fig. 3, microarc oxidation, fluoride treatment, dip coating, electrodeposition, anodization are the common forms of surface treatments for enhancing the corrosion resistance properties of Mg alloys which can be microgalvanic, intergranular, or transgranular.

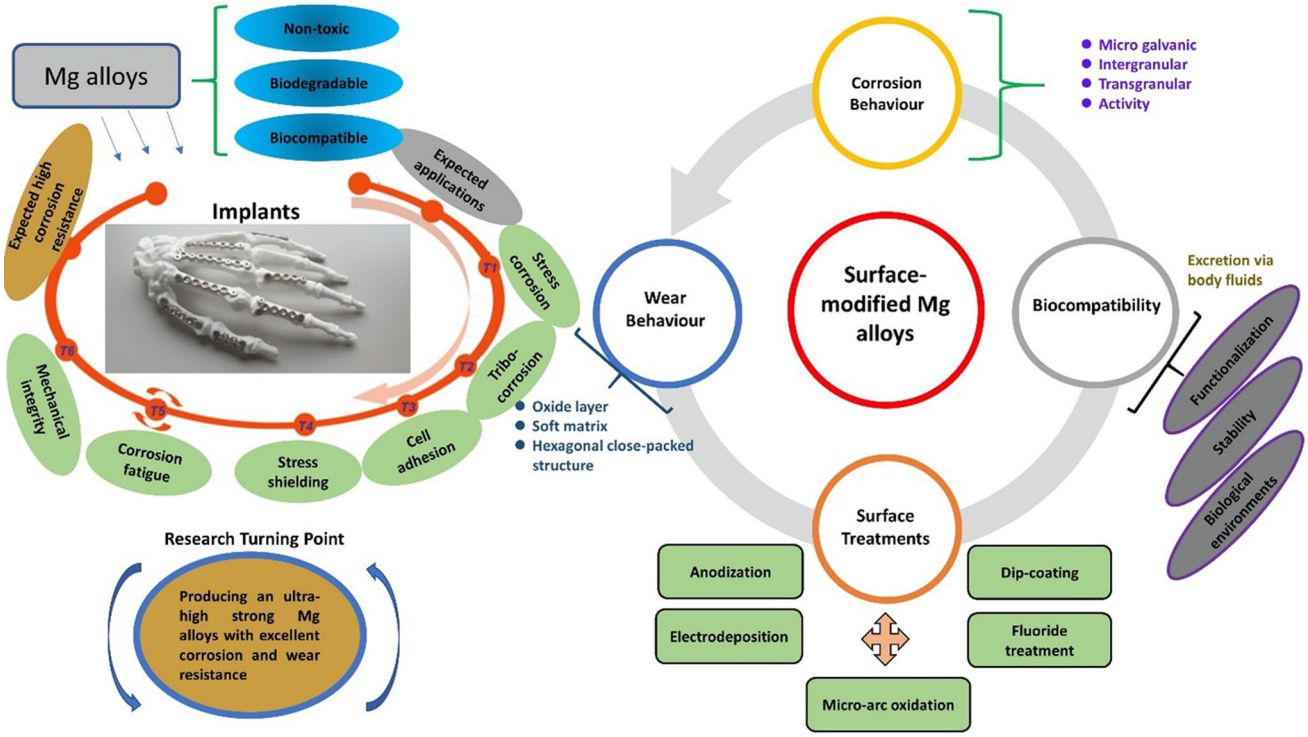

Fig. 3. Surface-modified Mg alloys—overview, properties, and applications

Over the years, surface nanocrystallization techniques including SMAT, shot peening, ultrasonic-assisted surface mechanical attrition, laser shock processing, air blast shot peening, etc. (Ref 43, 45-47) have also been adopted to improve the corrosion resistance. Surface gradient layers of few nanometers thick are often produced on the material surface as a result of the continuous bombardment of the material surface with a high-velocity fast-moving random balls. For instance, in SMAT and shot peening (Ref 34, 41), the collision of the material surface with balls induces the compressive residual stress leading to the dislocation and rearrangement of the inherent chemical elements of the materials as well as the general activity of the material, thereby creating a pathway for nucleation to occur, and hence the free movement of some protecting elements such as Cr to the material surface. This creates a Cr-rich surface layers, hence protecting the surface against external attack, especially when exposed to some aggressive environments. Furthermore, it is logical to say that surface nanocrystallization leads to the generation of nanometer-scale passive film resulting in lower corrosion current density and higher corrosion potential and impedance; hence, an enhanced corrosion resistance is expected. The corrosion resistance mechanism may be directly linked to the grain refinement and lower surface roughness obtained during the surface treatment (Ref 47).

Furthermore, the extent of surface nanostructuring can be controlled depending on the various treatment parameters including the ball size and material as well as the quantities of the balls. These parameters can be fine-tuned to suit a specific demand. For instance, using small ball and soft balls tends to reduce the surface roughness, thereby reducing the rate of corrosion. Without altering the chemical compositions, the nanocrystallized surface is often characterized with an enhanced potential polarization behavior, high interfacial density, and refined grains (Ref 41, 75).

Bimetal composites including Mg/Cu, Mg/Mg, Al/Al, Mg/Al, Cu-steel, etc. (Ref 71, 90-92, 95) are also good promising candidates for corrosion enhancement in Mg alloys due to their outstanding strength and properties. This can be attributed to the combined properties obtained from the metallurgically bonded metal components which will be difficult to obtain with the individual constituent element. Ideally, the inclusion of rare earth (RE) elements in the Mg alloys potentially enhance the corrosion resistance due to their inherent excellent corrosion-resistant ability. However, the presence of bimetal composites obtained from the combination of RE and biocompatible phases (Ref 71, 95) tends to further strengthen the Mg alloys in terms of corrosion resistance properties. This is possible in that the deficiency of one of the combining elements will be addressed by a superior element. For instance, in Cu-steel bimetal composites, the presence of Cu tends to increase strength and passivation ability, hence increasing the corrosion resistance properties.

5.1 Anodization

Through anodization via several electrolytes such as oxalic acid, chromic acid, and sulfuric acid solutions (Ref 98, 99), the surface chemistry of Mg alloy substrate can be changed by the generation of coating oxide on the surface and hence an improved esthetic qualities and resistance to most forms of corrosion including atmospheric and marine corrosions. However, the very poor thermal conductivity remains the main bottleneck during the anodization process of Mg alloy.

It is important to note that the anodization processing parameters or conditions including the anodizing time, voltage, temperature, current density, and electrolyte concentration (Ref 99-104) have a significant influence on the structure and morphology of the coating film formed, as well as the overall properties of the anodized materials. More importantly, the

coating thickness is directly linked with the anodizing time and temperature. For instance, low electrolyte solution can increase the film thickness up to about 8% (Ref 100), although the film thickness value may reduce if the electrolyte concentration increases beyond this value. However, this is not always the case as the maximum film thickness on the substrates can still be obtained at 10% electrolyte concentration (Ref 101). Furthermore, increasing the anodizing time up to 60 min (Ref 102) can increase the film thickness, and a further increase beyond 60 min may not have a noticeable influence on the film thickness. In aggressive solutions, an increase in the anodizing time reportedly increases the pore diameters (Ref 103, 104). The anodizing voltage plays an important part in the film characteristics including the barrier layer thickness, pore diameter and cell diameter. With lower anodizing voltages, thinner barrier layers, larger cell, and pore diameters can be achieved (Ref 105). Meanwhile, an increase in the current density can significantly enhance the mechanical properties of the protective coating on the material surface including the elastic modulus and hardness (Ref 106, 107). Increasing the anodizing temperature (not more than 25 °C) reportedly reduces the wear resistance and hardness of the protective coatings. However, increasing the anodizing temperature up to 50 °C (Ref 108) can enhance the pore diameter as well as the porosity and film growth.

5.2 Electrodeposition

As a form of corrosion protection methods for Mg alloys, the electrodeposition process depends to a large extent on some factors including the temperature, electrolyte pH, duty cycle, duration (time), and voltage (Ref 109-111). For instance, reducing the duty cycle can increase the hydrophobicity and reduce the coating surface roughness and thickness (Ref 109). In addition, by increasing the time, the corrosion current density can be reduced (Ref 112, 113) and the hydrophobicity and thickness of coating can be increased, whereas an increase in voltage can lead to reduction in the surface roughness of the coating (Ref 112).

To improve the corrosion properties of Mg alloys for biomedical applications, adopting any of the corrosion protection method is desirable. However, the combination of two or more corrosion methods can further enhance the corrosion resistance behavior (Ref 114, 115). Using aqueous electrolytes, several metals and alloys including Zn-Ni, Zn-Sn, Cu-Ni, and pure metals (Zn, Ni, Cu) can be electrolytically deposited on Mg alloy for corrosion protection.

5.3 Dip Coating

The corrosion resistance of Mg and its alloys as well as other metallic materials including Ti and Zn can also be improved by adopting dip coating method via the fabrication and deposition of organic and inorganic thin films/coatings including TiO_2, ZrO_2, Al_2O_3, and silica sol–gel (Ref 112, 116, 117) on the surface of Mg and its alloy with the aim of significantly increasing their corrosion resistance and adhesive strength for wider applications. With dip coating process, different forms of nanometric and homogenous films including biofilms, multilayer structures, polymeric layers, and sol–gel can be adequately deposited on the material surface for corrosion protection purpose.

Although the corrosion resistance and adhesive strength of Mg alloy can be greatly enhanced by dip coating process via the formation of inorganic coatings of the material surface, the process also suffers some setbacks including the formation of microcracks and pores on Mg surface resulting from the inorganic coatings preparation. This is probably attributed to the drying or sintering process at high temperature (Ref 118). Meanwhile, the resulting microcracks can be lightly reduced via ultraviolet-assisted treatment and pre-treatment. In addition, the process can block the screen creating a great impact in the final coating layer, and it is also slow. Furthermore, the organic coatings produced during dip coating process are often characterized with poor adhesion, thermal instability, and mechanical strength (Ref 118).

To achieve the formation of optimized active coating layers for effective corrosion protection, certain processing parameters such as the temperature, solution concentration, organic solvent selection (electrolyte), time duration, current mode (direct current, alternating current, bipolar, and unipolar modes), and current density, need to be properly considered during the dip coating process (Ref 119, 120). These processing parameters directly influence the coating properties including the thickness and composition, and the resulting corrosion and wear properties.

5.4 Microarc Oxidation

For corrosion protection of Mg alloys, there is a need to carefully select the process parameters for the microarc oxidation (MAO) process, which is also known as electrolytic plasma oxidation or plasma electrolytic oxidation. The microarc oxidation process as a means of enhancing the corrosion properties of Mg alloys offers better surface quality and enhancement and differs in many ways when compared to other surface treatment methods including the friction stir processing (FSP), sol–gel films (SGF) method, chemical and physical vapor depositions (CVD and PVD), plasma spraying (PS), laser surface modification (LSF), etc. (Ref 121-126). For instance, FSP enhances the wear and corrosion resistance, and biofunctionality, but cannot be applied on complex geometry due to low flexibility and processing rate (Ref 123). This limitation can be addressed by adopting MAO technique since it is suitable for coating of complex geometry and shapes without jeopardizing the quality and good surface finish (Ref 124). In SGF method, the coating thickness is hard to control and there is limitation of bioactivity as well as low adhesion strength between the substrate and the coating. MAO offers better bonding strength between the coating and the substrate, and good biocompatibility can be assured. Furthermore, a strong adhesion between the coating and substrate can be obtained and high-density coating can be produced with CVD and PVD. However, there is a problem of mismatch in mechanical features of the coating and that of the substrate which sometimes result in delamination (Ref 122). Even though a coating with an improved thermal stability, wear resistance, and biocompatibility can be obtained in plasma spraying (PS) (Ref 125), there is a possibility of experiencing weaken bonds and cracks as a result of the tensile forces formed between the coating and substrate. Meanwhile, there is no issue like delamination and weakened bonds in MAO as experienced in CVD, PVD, and PS since there is a perfect match and compatibility between the substate and coating and hence good mechanical and corrosion properties. In LSF, the corrosion and wear resistance of metals including Mg and Ti can be achieved, but there is also a problem of residual stress and low bond

strength resulting in the formation of cracks in laser-treated coatings (Ref 126). However, these issues can be adequately addressed thanks to microarc oxidation method through which a compact, dense, protective, and gradient-structured coatings (Ref 127, 128) can be produced on Mg alloys and other metallic materials.

The common microarc oxidation process parameters necessary to form and control excellent coatings on the surface of Mg alloys include the electrolyte concentration and compositions, duty cycle, treatment time, pulse frequency, voltage, and current density (Ref 121). These processing parameters can significantly influence the quality, microstructure, surface wettability and roughness, pore diameter, topography, and compositions of the microarc oxidation coatings deposited on Mg alloys, thereby affecting the functional, corrosion, physical, and mechanical properties of the Mg alloys for biomedical applications.

The treatment time is another important processing parameter influencing the coating properties during microarc oxidation process. Basically, the coating thickness increases with increasing treatment time up to a critical level, a further increase in the treatment time beyond the critical level may decrease the coating thickness and the coatings may become rougher at higher treatment time. In an investigation involving the enhancement of the corrosion properties of AZ31 Mg alloy by adopting microarc oxidation method using several treatment times (Ref 129), an increase in the treatment time from 1 to 5 min reportedly increased the coating thickness from 5 to 20 μm. However, the coating thickness decreases when the treatment time was increased to 8 min. To sum it up, high treatment time increases the coating roughness and the diameter of the micropores, thereby increasing the surface area, and hence reduced corrosion resistance. In addition, the spark discharge during the MAO process receives more power, thereby moving slowly on the material surface, and hence the fabrication of non-uniform coatings. Apart from the applied voltage, current density, treatment time, and nature of electrolytes, the duty cycle also influences the general performance and properties of the coatings in MAO process. Increasing the duty cycle reduces the coating thickness and increases the porosity. In short, the spark energy density and the amount of heat expended increase with an increase in duty cycle (Ref 130). Meanwhile, the frequency during the microarc oxidation process is directly linked with the pulse. That is, the strength of cathode pulse can be enhanced with increase in frequency (Ref 131). Increasing the frequency reduces the porosity and results in the formation of a compact and uniform coating with fine surface finish (Ref 132).

The electrolyte concentration and compositions are often linked with the bioactivity, phase components, and morphology of the coatings. In a recent study (Ref 133) investigating the influence of electrolytes on the coating properties via the use of different electrolytes and compositions, the solution containing glycerophosphate disodium salt pentahydrate and acetate monohydrate was reportedly adjudged the best exhibiting bioactivity with improved surface properties, as compared with other electrolytes (sodium phosphate and carbonate, and acetate monohydrate). This can be attributed to the high biocompatibility exhibited by the solution mixtures which enhance the bonding strength between the coating and the substrate, promoting rapid metal passivation, and hence reduced rate of corrosion. Generally speaking, phosphate (Ref 134, 135) and silicate (Ref 136, 137) electrolytes are the most common types of electrolytes used during the microarc oxidation process of metallic materials. Depending on the reaction between Mg^{2+} in Mg alloys and ions in electrolytes (Ref 138), there are wide differences between the two common electrolytes as regards the microarc oxidation process. While the silicate electrolytes are associated with the low corrosion resistance, lower coating thickness, finer surface, thinner size distribution, higher number of large pores, the phosphate electrolytes exhibit higher porosity and thickness, higher surface roughness, smaller number of large pores with wider size distribution, and improved corrosion resistance (Ref 138-140). The enhancement in the corrosion resistance of the coatings in phosphate electrolytes can be attributed to the low hydrophilic nature of the microarc oxidation coating leading to higher contact angle, the high chemical stability obtained from the ions in phosphate electrolytes which strongly support the passivation activities hence improved corrosion resistance, and the high coating thickness (Ref 121, 138).

To a large extent, the uniformity and porosity of the microarc oxidation as well as the thickness of the dense layer directly determine the extent of corrosion damage in Mg alloys (Ref 141). Microarc oxidation is a promising means of improving the corrosion resistance of Mg alloys with many merits such as high bond strength and the relieve of the residual stress (Ref 142-150). Despite its good sides, microarc oxidation also suffers some setbacks including the high porosity induced by the coatings which is capable of increasing the surface area, and hence increasing the corrosion rate (Ref 141-143, 149). To further enhance the corrosion resistance of Mg alloys, the microarc oxidation process in alkaline silicate solutions (Ref 136) or simulated body fluid (Ref 132) can be combined with other surface treatments (Table 4) such as electrophoresis process (Ref 145), polymer layer (Ref 144), and high-intensity pulsed ion beam (Ref 137). Applying microarc oxidation alone can improve protect the Mg alloy surface against corrosion, hence improving its corrosion resistance behavior. However, combining it with other treatments and solutions can further enhance the corrosion resistance behavior. The essence of combining two or more treatments together is that the surface treatments can complement each other in that the deficiency of one can be adequately catered for by another.

From the author's perspective, the structural features including the size, number of micropore, atomic ration, and thickness of the microarc coating are directly linked with the voltage applied during the MAO process. That is, the structural parameters increase with increasing applied voltage. However, the coating thickness is only directly affected by the time processing. Due to the reaction between the Mg alloy and oxygen, the interface bonding and bonding strength between the coating layer and the Mg substrate can be greatly enhanced with an increase in current density and applied voltage. Furthermore, the oxidation potential tends to increase with increasing current density and applied voltage resulting in the formation of dense coating layers with increased thickness. However, increasing the applied voltage above the critical limit may increase the porosity in the coating which may increase the surface roughness and subsequently increase the corrosion rate.

Anodization is one of the important surface pre-treatment processes for the corrosion protection of Mg alloy. Though ideally suited to aluminum (Al) and Al alloys (formation of protective strong Al_2O_3 on Al surface for corrosion protection purpose), the process can also be applied on other nonferrous

Table 4. Combined surface treatments on Mg alloys

S/N	Mg alloys	Surface treatment combinations	Benefits	References
1	AZ31B Mg alloy	Microarc oxidation alone	Resistant to corrosion, wear, and heat	130
2	AZ31 Mg alloys	Microarc oxidation alone	Enhanced alloy characterized with good coating properties and high hardness	146
3	AZ31 Mg alloys	Microarc oxidation + electrophoresis process	Surface chemistry of Mg alloy substrate can be changed by the generation of coating oxide	145
4	AZ31 Mg alloys	Plasma electrolytic oxidation + Polymer layer	Results in a stronger product, due to crystallization	144
5	Al-Cu-Mg alloy	Microarc oxidation alone	It makes the alloy more resistant to wear, heat, and corrosion	142
6	AZ31 Mg alloy	Plasma electrolytic oxidation alone	Weaker and cheaper alloy become stronger	140
7	AZ31 Mg alloy	Microarc oxidation	Pre-treatment is much simpler	138
8	Mg alloy	Microarc oxidation + high-intensity pulsed ion beam	Provides a clean process	137
9	Mg alloy	Microarc oxidation in alkaline silicate solutions	Provides chemical stability	136
10	AZ31 alloy	Microarc oxidation in simulated body fluid	Ceramic incorporates properties from electrolytes	132

metals including Mg. By the formation of thin-layer coating on electrodes through electrodeposition process, thin layers of functional materials including alloys and metals can be electrolytically deposited on the surface of Mg alloys (acting as the cathode in the electrolytic cell) with the aim of improving the corrosion properties and the overall mechanical behavior. Surface treatment by electrodeposition method can be generally categorized into pulse and direct electrodeposition (Ref 109). While the latter is performed under direct current where a constant current is generated in the electrolytes from the power supply to produce a compact and thin film, the former can be achieved by significantly reducing the additives in the electrolyte using a pulsed direct current to produce a high-purity thin-layer crystalline and uniform coating.

Compared to other surface treatment methods such as spray coating, dip coating process offers many advantages such as flexibility in adjusting the layer thickness, low cost, rapid and single pass formation of free pinhole coating layer. In addition, dip coating process is preferably secure, fast, and simple as compared to other coating methods. Depending on the withdrawal speed, immersion time and speed, the dip coating process can be generally summarized in five ways in sequential order: (1) immersion of the substrate into a desired solution at a constant immersion rate, (2) commencement of the pulling up of the dipped substrate from the solution after some time, (3) deposition of the film on the substrate after pulling up, (4) drainage of excess liquid from the material surface, and (5) evaporation of the solvent from the liquid film that is deposited on material surface. Dip coating is a well-known method for the production of stable perovskite solar cells (PSC). Usually, the surface tension, gravitational force, viscous drag, and force of inertia are the principal forces that are employed for the dip coating process. On the other hand, microarc oxidation is one of the most effective techniques to reducing the rate of corrosion of Mg/Mg alloys and other metallic materials and is presently receiving wide attention as an important means of corrosion protection. The oxide coatings formed on the metal surface are usually characterized with less defects on surface, high corrosion resistance and hardness, and excellent wear resistance.

6. Corrosion of Mg Alloys

The corrosion rates of Mg alloy depend to a large extent on some important factors including the weak passive hydroxide film generated on Mg alloy, texture, dislocations, lattice defects like grain boundaries, impurities or defects, and internal galvanic corrosion induced by second phases (Ref 5, 88, 151).

The potentiodynamic polarization showing the comparison between the corrosion current density and potentials of Mg alloys in 0.6 M NaCl at room temperature (25 °C) is summarized in Table 5. The corrosion properties of Mg can be evaluated using the corrosion current density and potential. As indicated in Table 5, $Mg_{66}Zn_{30}Ca_4$, $Mg_{70}Zn_{25}Ca_5$, and AZ91 alloy exhibited the corrosion current densities of 3.53 $\mu A/cm^2$ (Ref 92), 11.2 $\mu A/cm^2$ (Ref 92), and 25.5 $\mu A/cm^2$ (Ref 151), respectively. It is generally believed that the lower the corrosion current density, the higher the formation of the passive films and hence higher corrosion resistance. Likewise, the higher the corrosion potential the better the corrosion resistance.

In addition, the Mg metal with a higher corrosion potential of 1.620 V (Ref 151) is expected to have an enhanced corrosion resistance behavior when compared with Mg-Zn-Ca-0.0Ce/La (Ref 159), Mg alloy ZAXM42 (Ref 160), and Mg-15HA (Ref 152) with corrosion potentials of − 1.553, − 1.431, and − 0.872, respectively (Table 5). The $Mg_{66}Zn_{30}Ca_4$ alloy is expected to possess high corrosion resistance since it has the lowest corrosion current density. The corrosion properties can be determined using the potentiodynamic and potentiostatic polarizations, the immersion test, or Mott–Schottky analysis. The reference electrode (RE) during the electrochemical tests can be saturated calomel electrode (SCE) or silver/silver chloride (Ag/AgCl) while the counter electrode (CE) can be platinum (Pt) or graphite rod (Ref 42, 46). It is worth studying the effects of reference electrode on the corrosion resistance properties of Mg alloy. This is because the usage of Ag/AgCl will definitely have a different effect on the corrosion resistance of Mg alloy as compared to SCE. Furthermore, using a very small scan rate let us say 0.1 mV/s tends to capture very well the corrosion resistance process compared to using large scanning rate of about 1 mV/s.

The corrosion morphology of a typical Mg alloy revealing the influence of corrosion on the microstructure with the presence of some corrosion products and cracks on different parts of the sample after potentiodynamic polarization in 3.5 wt.% NaCl aqueous solution at room temperature is illustrated in Fig. 4. When exposed to aggressive and physiological environments, Mg alloys tend to degrade with gradual breaking down of the protective passive layer, leading to the formation of corrosion products. As observed in Fig. 4, crack initiation also set in which later propagate to other parts of the material leading to fracture or total failure.

In an electrochemical property investigations of Mg alloys (Fig. 5), the Mg alloy subjected to surface treatment by magnetron sputtering using MgZnCa coating exhibits a higher corrosion potential than the pure Mg. In addition, compared to the pure Mg with a corrosion current density of 21.110 mA/cm^2, the coated Mg alloy can exhibit a reduced corrosion current density of 15.656, 13.678, and 7.712 mA/cm^2 for Mg alloy coated for 20, 40, and 60 min, respectively. In addition, when compared with the pure Mg with a more negative corrosion potential of − 1.326, the nobler potential of − 0.853 V (Fig. 5) exhibited by the Mg alloy coated for 60 mins indicates that the corrosion potential is high, hence emphasizing the vital role played by surface treatment in supporting passivation and reducing corrosion to the minimum.

It is well known that the lower the corrosion current density, the more the formation of a compact protective passive film on the sample surface, and hence the better the corrosion resistance. Hence, the coated Mg alloys are better in terms of corrosion resistance and the corrosion resistance increases with coating thickness. Generally, the corrosion of Mg alloys is determined to a large extent by the corrosion current density and potential as well as the electrochemical impedance. It is generally believed that the more positive and nobler the corrosion potential (Fig. 6), the higher the corrosion resistance property because the nobler corrosion potential means the material sample has a higher tendency of resisting corrosion attack.

When the corrosion current density is reduced, the electron mobility tends to reduce, reducing the reaction and interaction of the material sample with the corrosive medium, hence preventing external attack leading to improved corrosion resistance property. When corrosion sets in, corrosion products and cracks appear on different parts of the sample leading to corrosion and corrosion fatigue under the combined action of repeated stress and corrosion reaction. The corrosion attack often starts from the surface and edges, and later spread into the material like a few nanometers thick, thereby affecting the microstructure of the material. So mostly, many corrosion experts and material specialists often adopt surface treatment methods in a bid to improve the corrosion resistance so as to sustain the application of Mg alloy for biomedical implants.

7. Mechanical Properties: Corrosion Rates Synergy

Producing an ultra-high and strong Mg alloy with exceptional yield strength without jeopardizing the ductility (Fig. 7) is the dream of many material scientists and corrosion experts. The yield strength–elongation relationship (Fig. 7) reveals that some Mg alloys at room temperature like AZ31 (Ref 59, 113), AZ61 (Ref 51, 52), and Mg-Zn-Ge (Ref 73) can exhibit high yield strength of about 190, 185, and 160 MPa, respectively, with good elongation. With elongations of 27% for Mg-Zn-Y-Nd, and 25% for Mg0.5Zn0.2Ca, both Mg alloys can be regarded as ductile as indicated by the trend in Fig. 7. Meanwhile, AE42, Mg-3Al-1Zn, and DieMag422 alloys with elongations of 6%, 2%, and 1%, respectively, can be regarded as brittle alloys. More importantly, developing mechanically sound Mg alloys with excellent corrosion and wear resistance is of utmost priority. Several efforts have been made in the past to achieve this including alloying, surface nanocrystallization, and surface treatments. By this, the mechanical properties of Mg alloys are improved without trading off the corrosion resistance.

The relationship between the mechanical property (yield strength (YS)) and the corrosion rates of several Mg alloys including Mg-Sn-ST (Ref 161), Mg-Zn (Ref 153), Mg-Mn (Ref 161), Mg-Ca-C (Ref 161), Mg-Zn-Ca-Ce (Ref 160), Mg-Sr (Ref 154), WE43 (Ref 53, 155, 157), AZ91 (Ref 18), etc. has been investigated in the past and is summarized in Fig. 8.

For instance, the YS of Mg-Zn-Ca alloy (Ref 160) was reported to be 220.2 MPa with the corrosion rate of 0.41 mm/y, whereas the corrosion rate of Mg alloy WE43 (Ref 53) is 0.39 mm/y with a YS of 215 MPa. Meanwhile, the Mg-0.3Ca-C, Mg-1Ca, and Mg-1Zn alloys possessed reduced yield strengths of 45, 40, and 25.5 MPa, respectively, with corrosion rate of 0.71 mm/year for Mg-0.3Ca-C, 12.56 mm/year for Mg-1Ca, and 1.52 mm/year for Mg-1Zn. The trends in Fig. 8 show that Mg-0.3Ca-C, Mg-1Ca, and Mg-1Zn can be regarded as weak alloys due to low YS, while Mg-Zn-Ca and WE43 are strong Mg alloys due to high YS. Under the continuous exposure of Mg alloy to corrosive environments without proper and adequate protection method in place, localized corrosion sets in making the corrosion rate of Mg alloy to be on the high side, hence affecting the surface microstructure as well as the mechanical properties, thereby leading to gradual deterioration in mechanical integrity. It is now the dream of many material scientists to produce an ultra-strong Mg alloy with excellent corrosion resistance–mechanical properties synergy, which can stand the test of time.

Table 5. Potentiodynamic polarization—comparison between the corrosion current density and potentials of Mg alloys in 0.6 M NaCl at room temperature (25 °C)

Mg alloys	i_{corr}, $\mu A/cm^2$	E_{corr}, V	Scan rate, mV/s	Scan range, V	Medium	CE	RE	EIS signal, mV	Temp, °C	References
Mg metal	5.50	1.620	1	−0.15 to +1.5	3.5 wt.% NaCl	Pt	SCE	10	25	151
AZ91 alloy	25.5	1.505	1	−0.15 to +1.5	3.5 wt.% NaCl	Pt	SCE	10	25	151
AZ31 alloy	90.0	1.540	1	−0.15 to +1.5	3.5 wt.% NaCl	Pt	SCE	10	25	151
AZ91	730.0	− 1.75	5	− 0.25 to + 0.25	0.1 M NaCl				25	5
Pure Mg	549.2	− 1.526	2	− 0.2 to + 0.2	SBF	Pt wire	SCE	5	25	88
Mg-MMC	95.02	− 1.475	2	− 0.2 to + 0.2	SBF	Pt wire	SCE	5	25	88
Mg66Zn30Ca4	3.53	− 1.235	1	− 0.3 to + 4	SBF	Pt	SCE		37	92
Mg70Zn25Ca5	11.2	− 1.322	1	− 0.3 to + 4	SBF	Pt	SCE		37	92
as-rolled pure Mg	36.8	− 1.750	1	− 0.3 to + 4	SBF	Pt	SCE		37	92
AZ31 alloy	106.0	− 1.31	0.5	− 0.2 to + 0.6	SBF	Graphite	SCE	10	36.5	129
AZ91	4.51	− 1.50			3.5 wt.% NaCl	Pt plate	Ag/AgCl		25	131
AZ31	101	− 1.30	3		SBF	Graphite rod	SCE	10	36.5	132
AZ31	1.5	− 1.64	5		SBF	Pt sheet	SCE			145
ZE41	90		0.2		1 M NaCl		SCE		25	141
AZ91D	40		0.2		1 M NaCl		SCE		25	141
Pure Mg	120		0.2		1 M NaCl		SCE		25	141
Mg-15HA	3.397	− 0.872	5	−1.5 to + 0	3.5% NaCl	Graphite	SCE		30	152
Mg-10HA	2.67	− 0.939	5	−1.5 to + 0	3.5% NaCl	Graphite	SCE		30	152
Mg-8HA	4.387	− 1.434	5	−2.0 to + 0	3.5% NaCl	Graphite	SCE		30	152
M-Mg	20.987	− 1.586	5	−2.0 to + 0	3.5% NaCl	Graphite	SCE		30	152
Mg alloy ZAXM4211	17.1	− 1.431			3.5 wt% NaCl + $Mg(OH)_2$					159
Mg-Zn-Ca-0.0Ce/La	17.99	− 1.569	5	− 0.4 to + 0.1	3.5 wt% NaCl	Pt	SCE		25	160
Mg-Zn-Ca-0.5Ce/La	68.49	− 1.487	5	− 0.4 to + 0.1	3.5 wt% NaCl	Pt	SCE		25	160
Mg-Zn-Ca-1.0Ce/La	37.97	− 1.553	5	− 0.4 to + 0.1	3.5 wt% NaCl	Pt	SCE		25	160
Mg-0.3Ca-C	31	− 1.601	0.6	− 0.25 to + 0.02	3.5% NaCl + Mg $(OH)_2$	Pt	Ag/AgCl/Sat KCl	8	25	161
Mg-5Sn-ST	154	− 1.519	0.6	− 0.25 to + 0.02	3.5% NaCl + $Mg(OH)_2$	Pt	Ag/AgCl/Sat KCl	8	25	161
Mg-1.0Mn-R	99	− 1.546	0.6	− 0.25 to + 0.02	3.5% NaCl + $Mg(OH)_2$	Pt	Ag/AgCl/Sat KCl	8	25	161
Mg-5.0Sn-R	120	− 1.514	0.6	− 0.25 to + 0.02	3.5% NaCl + $Mg(OH)_2$	Pt	Ag/AgCl/Sat KCl	8	25	161
Mg-5.0Zn-ST	303	− 1.486	0.6	− 0.25 to + 0.02	3.5% NaCl + $Mg(OH)_2$	Pt	Ag/AgCl/Sat KCl	8	25	161
Mg-0.3Ca	68.6	− 1.579	0.6	− 0.30 to + 0.03	3.5% NaCl + $Mg(OH)_2$	Pt	Ag/AgCl/Sat KCl		25	162
Mg-6.0Al	30.3	− 1.573	0.6	− 0.30 to + 0.03	3.5% NaCl + $Mg(OH)_2$	Pt	Ag/AgCl/Sat KCl		25	162
High-purity (HP) Mg	10.2	− 1.631			3.5% NaCl + $Mg(OH)_2$				25	163
Mg-2.0Dy-0.1Zn	19.32	−1.566	1		3.5 wt.% NaCl	Pt	SCE		25	164

*CE counter electrode, *RE* reference electrode

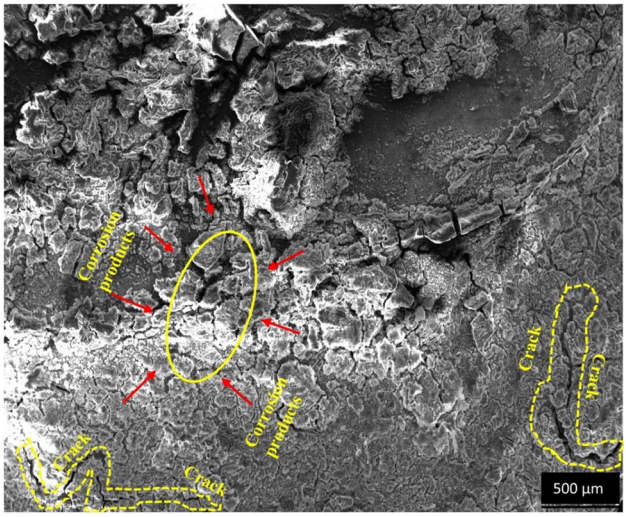

Fig. 4. Corrosion morphology of a typical Mg alloy revealing the influence of corrosion on the microstructure with the presence of some corrosion products and cracks on different parts of the sample after potentiodynamic polarization in 3.5 wt.% NaCl aqueous solution at room temperature

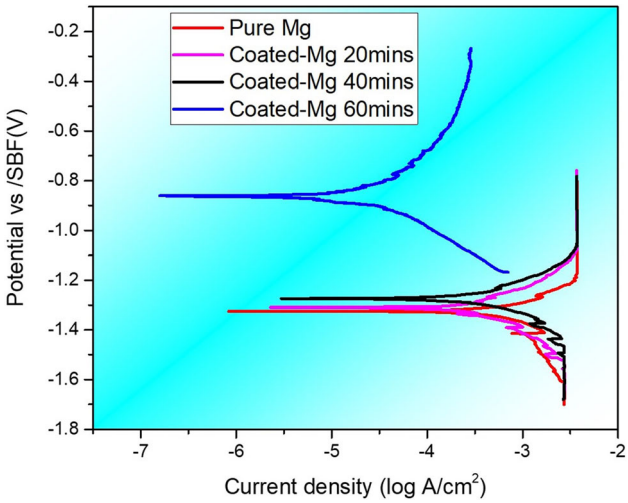

Fig. 5. Corrosion resistance behavior of pure Mg and coated Mg alloys for 20, 40, and 60 min, after polarization from their respective open-circuit potentials in simulated body fluid (SBF) at 37 °C

8. Effect of Texture on Corrosion and Fatigue Properties

Apart from grain refinement and residual stresses, texture evolution and orientation to a large extent have a significant influence on the corrosion and corrosion fatigue properties of Mg alloys (Ref 165-174). Deformation texture which can be fiber texture or basal texture is common with Mg alloys and largely depends on the processing methods. For instance, the fiber texture can be formed by extrusion and basal texture by rolling (Ref 167). As observed in extruded AM60 Mg alloy (Ref 165), due to its high atomic density, the basal plane of grains exhibits a higher corrosion resistance leading to a lower surface energy and an increase in the uniformity of surface

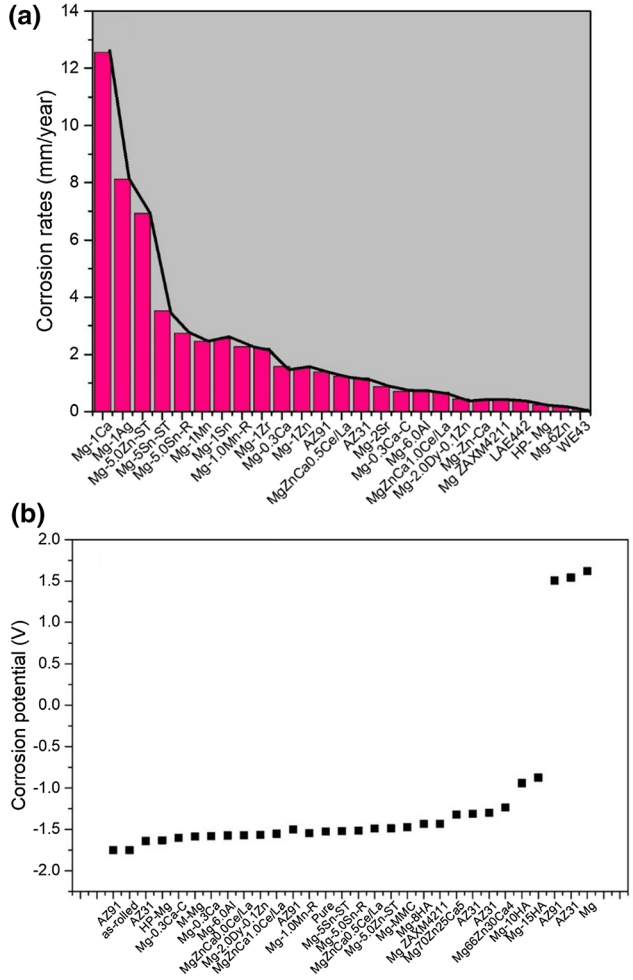

Fig. 6. Summary of the corrosion rates and potentials of various Mg alloys: (a) corrosion rates (mm/year) and (b) corrosion potential (V) (data compiled from (Ref 92, 145, 153-157, 159-164)

energy, as compared with its non-basal plane counterpart. The twinning texture improves the protective ability of the corrosion film and hence an enhanced corrosion resistance of AM60 Mg alloy. In addition, an improvement in the uniformity of the surface energy promotes the formation of uniform and compact oxide corrosion-free film, i.e., the more pronounced the texture orientation, the higher the uniformity of the surface energy and the better the corrosion resistance behavior. The influence of texture on the corrosion and fatigue properties of Mg alloys is illustrated in Fig. 9 (Ref 171-173).

Attributed to its lower polarization current densities, the strongly basal-textured grain orientation induced by plastic deformation significantly improves the corrosion properties of AZ31B Mg alloy (Ref 171). The depth is directly proportional to the texture evolution, i.e., the basal texture increases with increasing depth. As indicated in Fig. 9(a) (Ref 171), the basal peak reduces when the depth changes from 6 to 2 mm, and no basal texture is observed when the depth is further reduced to 0.5 mm. The maximum texture intensity (TD) is another important factor influencing the corrosion properties. The (0 0 0 2) pole figure revealing the crystallographic texture of ZK60 Mg alloy at different TD is shown in Fig. 9(b) (Ref 172). The dominant texture with basal planes parallel to extrusion direction (ED) reduces in strength as the TD increases from

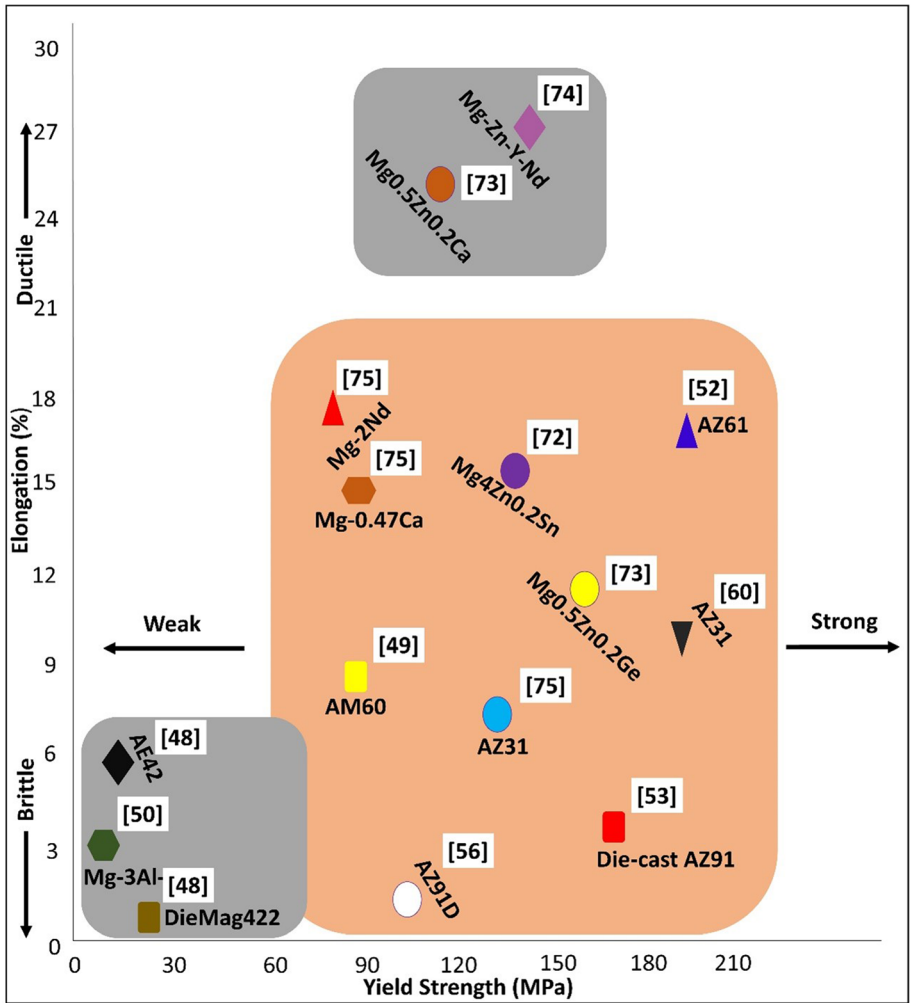

Fig. 7. Yield strength–elongation relationship of selected Mg alloys at room temperature (data compiled from (Ref 48, 49, 51, 52, 56, 57, 59, 73-75, 113)

5.7 to 9.2. Investigating the influence of texture on the fatigue strength of extruded AZ61 Mg alloy (Ref 173) (Fig. 9c), texture has no significant effect on the fatigue strength at higher stress amplitude level. However, at $<$ 90 MPa, the longitudinal AZ61 Mg alloy exhibited a higher fatigue strength of 85 MPa compared to 67 and 63 MPa possessed by the 45° and transverse AZ61 Mg alloy samples. By this, the fatigue properties of AZ61 Mg alloy are significantly affected due to the dominant basal plane texture.

9. Summary and Future Work

Due to their special attributes such as non-toxicity, biodegradability, and biocompatibility, Mg alloys are the promising candidates for orthopedic implants and other biomedical applications. However, their useful applications and importance is constantly under threat because of their poor resistance to corrosion, especially under the combined action of repeated stress and aggressive corrosive environment. This often leads to loss of mechanical integrity in terms of tensile properties, limits the corrosion fatigue strengths and induces fatigue crack initiation from inclusions and defects in air and corrosion pits from solutions like simulated body fluid or Hank's solution. The loss in mechanical integrity is attributed to their weakness to localized corrosion. Hydrogen embrittlement, stress corrosion, and localized corrosion can also result in fatigue crack initiation in physiological environments.

Till date, surface treatment (anticorrosion processing) including microarc oxidation, dip coating, electrodeposition, anodization, etc., remains an important technique for the corrosion protection of Mg alloys. In addition, surface treatment does not only enhance the corrosion resistance properties of Mg alloys but also make them functionalized. Through the generation of protective layer on Mg surface during surface treatment, the Mg alloy–environment direct contact can be prevented. Several factors including the texture regulation, grain refinement, phase distribution, and grain boundary could influence the corrosion resistance property as well as the fatigue strength of Mg alloy whose mechanical properties resemble that of natural bone. Mg-based non-toxic materials can be integrated in human body, and by forming combined nanotexture and microtexture, the bone surface can be imitated.

Polarization method, weight loss method, hydrogen evolution method, rate of Mg^{2+} leaving the metal surface, EIS analysis, and immersion test are the common ways of evaluating the corrosion rates of Mg alloys; at least two or

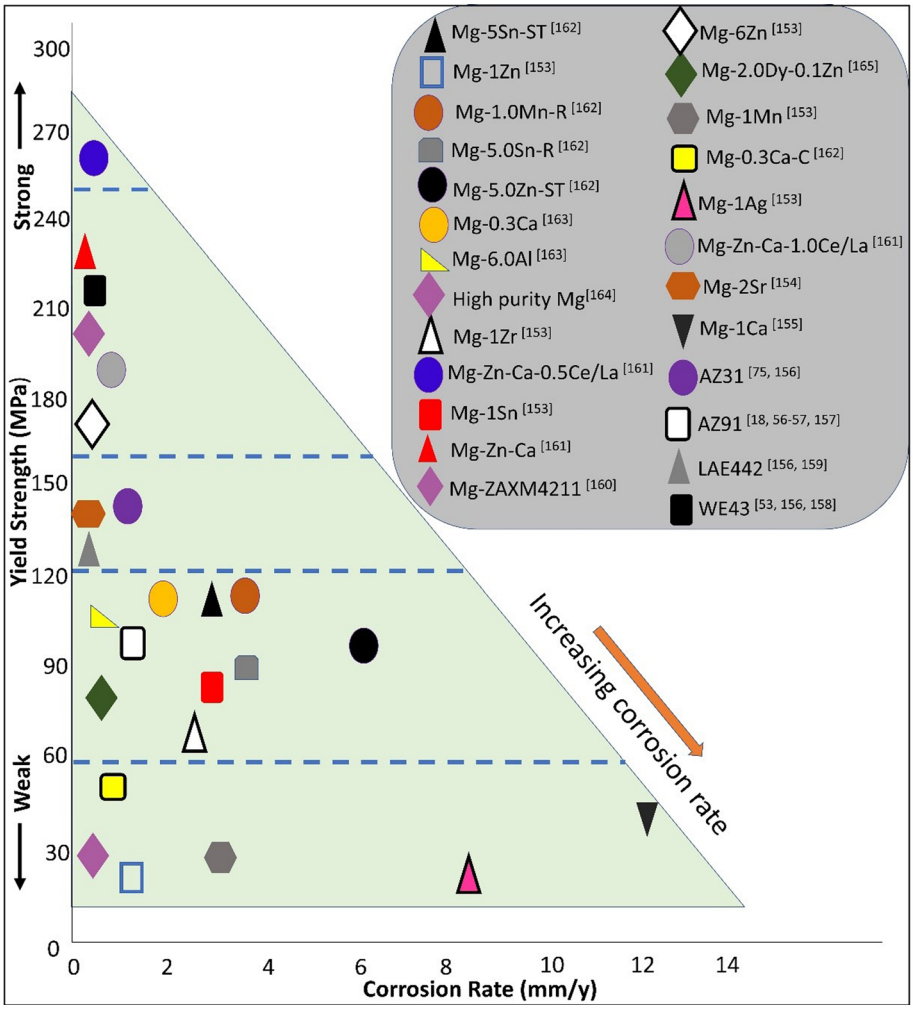

Fig. 8. Relationship between the mechanical property (yield strength) and corrosion rate of selected Mg alloys (data compiled from (Ref 53, 75, 153, 155, 157-160, 163, 164)

more of these methods should be adopted in adequately and effectively measuring the corrosion rate since the setbacks using one method say polarization method can be addressed by other methods such as hydrogen evolution and weight loss methods.

Ways to enhance the corrosion resistance properties include the integration of Mg composites with polymers and ceramics, alloying, and surface treatment. For future developments, the following can be considered. In our previous work (Ref 40), biodegradable behavior of perforated cannulated Mg hip stents was investigated via two treatment methods—machining and molding. In a bid to further improve the electrochemical properties, this research can be extended in future by investigating the influence of other surface treatments like rolling on the biodegradable behavior of Mg hip scents. Furthermore, the influence of texture with different orientation on the corrosion and fatigue properties of Mg alloys can be further investigated. The combined effects of three or more alloying elements (Al-Sn-Zn, Ca-Zn-Al-Si, Sn, Sr-Nd-Y-Ca-Zn) on the corrosion behavior of Mg alloys are yet to be fully explored and hence will serve as good subjects of investigations in future research on Mg alloys. This will help in identifying the most influencing alloying element as well as the optimum compositions of each element for better corrosion resistance. In addition, an extensive study is needed to fully investigate the relationship between the processing parameters during surface treatment and corrosion resistance behavior as well as the consequential effect on corrosion resistance. Biocompatible coating application and their means of overcoming the problem of corrosion fatigue in Mg alloys as well as the impact of stress corrosion cracking on corrosion fatigue crack propagation can also be looked into. Meanwhile, the corrosion fatigue behavior of Mg alloy (free of Al) in physiological environments which resemble the actual mechanical properties of human body still need further investigations. More importantly, the corrosion fatigue crack propagation investigations of Mg alloys in physiological environments and the influence of organic molecules on Mg alloy corrosion-induced cracking process should be carried out.

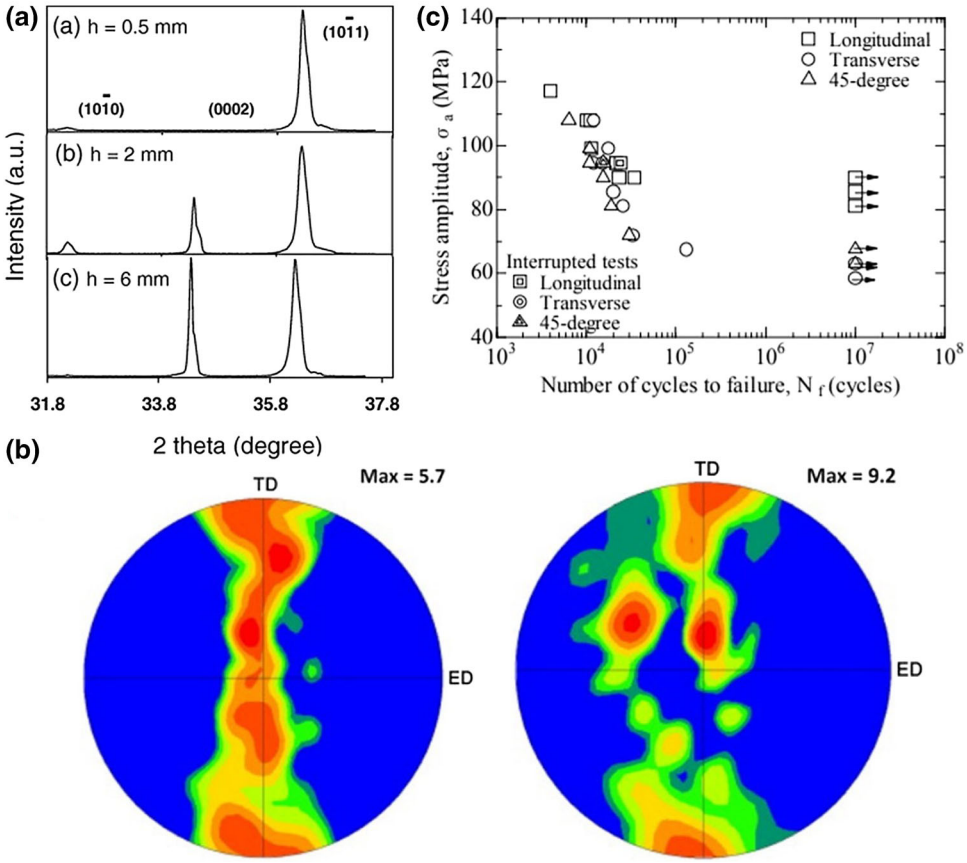

Fig. 9. Influence of texture on the corrosion and fatigue properties of Mg alloys: (a) texture effects on the lateral surface at different depth of AZ31B Mg alloy (reprinted from Ref 171, copyright 2011, with permission from Elsevier), (b) (0 0 0 2) pole figure showing the crystallographic texture of ZK60 Mg alloy (TD signifies maximum texture intensity, ED means extrusion direction) (reprinted from Ref 172, copyright 2014, with permission from Elsevier), (c) influence of texture on fatigue strength of extruded AZ61 Mg alloy (reprinted from Ref 173, Key Engineering Materials, Vol 274-276, 2004, p 193-198, "Effect of Texture on Fatigue Properties of an Extruded AZ61 Magnesium Alloy Plate," Z. Sajuri, Y. Miyashita, Y. Mutoh, Y. Hosokai, copyright 2004 TransTech Publications, with kind permission of TransTech Publications)

Declarations

Conflict of interest

The authors declare no conflict of interest.

References

1. P. Gunde, A.C. Hänzi, A.S. Sologubenko and P.J. Uggowitzer, High-Strength Magnesium Alloys for Degradable Implant Applications, *Mater. Sci. Eng. A.*, 2011, **528**, p 1047–1054
2. M. Niinomi, M. Nakai and J. Hieda, Development of New Metallic Alloys for Biomedical Applications, *Acta Biomater.*, 2012, **8**, p 3888–3903
3. Y. Okazaki and E. Gotoh, Metal Release from Stainless Steel, Co-Cr-Mo-Ni-Fe and Ni-Ti Alloys in Vascular Implants, *Corros. Sci.*, 2008, **50**, p 3429–3438
4. M.P. Staiger, A.M. Pietak, J. Huadmai and G. Dias, Magnesium and Its Alloys as Orthopedic Biomaterials: A Review, *Biomaterials*, 2006, **27**, p 1728–1734
5. R.K. Singh Raman, N. Birbilis and J. Efthimiadis, Corrosion of Mg Alloy AZ91—The Role of Microstructure, *Corros. Eng. Sci. Technol.*, 2004, **39**, p 346–350
6. N.-E.L. Saris, E. Mervaala, H. Karppanen, J.A. Khawaja and A. Lewenstam, Magnesium: An Update on Physiological, Clinical and Analytical Aspects, *Clin. Chim. Acta.*, 2000, **294**, p 1–26
7. F.I. Wolf and A. Cittadini, Chemistry and Biochemistry of Magnesium, *Mol Aspect Med.*, 2003, **24**, p 3–9
8. E. Ma and J. Xu, Biodegradable Alloys: The Glass Window of Opportunities, *Nat. Mater.*, 2009, **8**, p 855–857
9. B. Zberg, P.J. Uggowitzer and J.F. Loffler, MgZnCa Glasses Without Clinically Observable Hydrogen Evolution for Biodegradable Implants, *Nat. Mater.*, 2009, **8**, p 887–891
10. F. Witte, V. Kaese, H. Haferkamp, E. Switzer, A. Meyer-Lindenberg, C.J. Wirth et al., In Vivo Corrosion of Four Magnesium Alloys and the Associated Bone Response, *Biomaterials*, 2005, **26**, p 3557–3563
11. F. Witte, The History of Biodegradable Magnesium Implants: A Review, *Acta Biomater.*, 2011, **6**, p 1680–1692
12. F. Witte, J. Fischer, J. Nellesen, H.-A. Crostack, V. Kaese, A. Pisch et al., In Vitro and In Vivo Corrosion Measurements of Magnesium Alloys, *Biomaterials*, 2006, **27**, p 1013–1018
13. S.F. Kraus, A.C. Fischerauer, P.J. Hänzi, J.F. Witzer, A.M. Löffler and F. Weinberg, Magnesium Alloys for Temporary Implants in Osteosynthesis, *In Vivo Studies of Their Degradation and Interaction with Bone, Acta Biomater.*, 2012, **8**, p 1230–1238
14. M.B. Kannan and R.K.S. Raman, In Vitro Degradation and Mechanical Integrity of Calcium-Containing Magnesium Alloys in Modified-Simulated Body Fluid, *Biomaterials*, 2008, **29**, p 2306–2314
15. N. Kirkland, M. Staiger, D. Nisbet, C. Davies and N. Birbilis, Performance-Driven Design of Biocompatible Mg Alloys, *JOM.*, 2011, **63**, p 28–34
16. B. Heublein, R. Rohde, V. Kaese, M. Niemeyer, W. Hartung and A. Haverich, Biocorrosion of Magnesium Alloys: A New Principle in Cardiovascular Implant Technology?, *Heart*, 2003, **89**, p 651–656

17. N.T. Kirkland, J. Lespagnol, N. Birbilis and M.P. Staiger, A Survey of Bio-Corrosion Rates of Magnesium Alloys, *Corros. Sci.*, 2010, **52**, p 287–291
18. G. Song, Control of Biodegradation of Biocompatible Magnesium Alloys, *Corros. Sci.*, 2007, **49**, p 1696–1701
19. S. Jafari, R.K.S. Raman and C.H.J. Davies, Corrosion Fatigue of a Magnesium Alloy in Modified Simulated Body Fluid, *Eng. Fract. Mech.*, 2015, **137**, p 2–11
20. H. Amel-Farzad, M.T. Peivandi and S.M.R. Yusof-Sani, In-Body Corrosion Fatigue Failure of a Stainless Steel Orthopaedic Implant with a Rare Collection of Different Damage Mechanisms, *Eng. Fail Anal.*, 2007, **14**, p 1205–1217
21. B. Aksakal, Ö.S. Yildirim and H. Gul, Metallurgical Failure Analysis of Various Implant Materials Used in Orthopedic Applications, *J. Fail. Anal. Prev.*, 2004, **4**, p 17–23
22. C.R.F. Azevedo, Failure Analysis of a Commercially Pure Titanium Plate for Osteosynthesis, *Eng. Fail Anal.*, 2003, **10**, p 153–164
23. L. Choudhary and R.K.S. Raman, Magnesium Alloys As Body Implants: Fracture Mechanism Under Dynamic and Static Loadings in a Physiological Environment, *Acta Biomater.*, 2012, **8**, p 916–923
24. M.B. Kannan and R.K.S. Raman, Evaluating the Stress Corrosion Cracking Susceptibility of Mg-Al-Zn Alloy in Modified-Simulated Body Fluid for Orthopaedic Implant Application, *Scr. Mater.*, 2008, **59**, p 175–178
25. L. Choudhary, J. Szmerling, R. Goldwasser and R.K.S. Raman, Investigations into Stress Corrosion Cracking Behaviour of AZ91D Magnesium Alloy in Physiological Environment, *Proc. Eng.*, 2011, **10**, p 518–523
26. L. Choudhary and R.K.S. Raman, Mechanical Integrity of Magnesium Alloys in a Physiological Environment: Slow Strain Rate Testing Based Study, *Eng. Fract. Mech.*, 2013, **103**, p 94–102
27. L. Choudhary and R.K.S. Raman, Threshold Stress Intensity for Stress Corrosion Cracking (KISCC) of a Magnesium Alloy in Physiological Environment, *Mater. Sci. Forum.*, 2011, **690**, p 487–490
28. Y. Murakami and K.J. Miller, What is Fatigue Damage? A View Point from the Observation of Low Cycle Fatigue Process, *Int. J. Fatigue.*, 2005, **27**, p 991–1005
29. A. Winzer, W. Atrens, V.S. Dietzel, G. Raja, K.U. Song and U. Kainer, Characterisation of Stress Corrosion Cracking (SCC) of Mg-Al Alloys, *Mater. Sci. Eng. A*, 2008, **488**, p 339–351
30. M.B. Kannan, W. Dietzel, R.K.S. Raman and P. Lyon, Hydrogen-Induced-Cracking in Magnesium Alloy Under Cathodic Polarization, *Scr. Mater.*, 2007, **57**, p 579–581
31. T.E. Abioye, I.S. Omotehinse, I.O. Oladele, T.O. Olugbade and T.I. Ogedengbe, Effects of Post-weld Heat Treatments on the Microstructure, Mechanical and Corrosion Properties of Gas Metal Arc Welded 304 Stainless Steel, *World J. Eng.*, 2020, **17**, p 87–96
32. T.E. Abioye, T.O. Olugbade and T.I. Ogedengbe, Welding of Dissimilar Metals Using Gas Metal Arc and Laser Welding Techniques: A Review, *J. Emerg. Trends Eng. Appl. Sci. (JETEAS)*, 2017, **8**, p 225–228
33. T. Mohammed, T.O. Olugbade and I. Nwankwo, Determination of the Effect of Oil Exploration on Galvanized Steel in Niger Delta, Nigeria, *J. Sci. Res. Rep.*, 2016, **10**, p 1–9
34. T. Olugbade, J. Lu, Effects of Materials Modification on the Mechanical and Corrosion Properties of AISI 316 Stainless Steel. In *12th International Conference on Fatigue Damage of Structural Materials*, Cape Cod, Hyannis, USA (2018)
35. C. Dang, Y. Yao, T.O. Olugbade, J. Li and L. Wang, Effect of Multi-interfacial Structure on Fracture Resistance of Composite TiSiN/Ag/TiSiN Multilayer Coating, *Thin Solid Films*, 2018, **653**, p 107–112
36. C. Dang, T.O. Olugbade, S. Fan, H. Zhang, L.L. Gao, J. Li and Y. Lu, Direct Quantification of Mechanical Responses of TiSiN/Ag Multilayer Coatings Through Uniaxial Compression of Micropillars, *Vacuum*, 2018, **156**, p 310–316
37. T.O. Olugbade, T.E. Abioye, P.K. Farayibi, N.G. Olaiya, B.O. Omiyale and T.I. Ogedengbe, Electrochemical Properties of MgZnCa-Based Thin Film Metallic Glasses Fabricated via Magnetron Sputtering Deposition Coated on a Stainless Steel Substrate, *Anal. Lett.*, 2021, **54**, p 1588–1602
38. T.O. Olugbade, O.T. Ojo, B.O. Omiyale, E.O. Olutomilola and B.J. Olorunfemi, A Review on the Corrosion Fatigue Strength of Surface-Modified Stainless Steels, *J. Braz. Soc. Mech. Sci. Eng.*, 2021, **43**, p 421
39. T.E. Abioye, D.G. McCartney and A.T. Clare, Laser Cladding Of Inconel 625 Wire For Corrosion Protection, *J. Mater. Process. Technol.*, 2015, **217**, p 232–240
40. H. Zu, K. Chau, T.O. Olugbade, L. Pan, D.H. Chow, L. Huang, L. Zheng, W. Tong, X. Li, Z. Chen, X. He, R. Zhang, J. Mi, Y. Li, B. Dai, J. Wang, J. Xu, K. Liu, J. Lu and L. Qin, Comparison of Modified Injection Molding and Conventional Machining in Biodegradable Behavior of Perforated Cannulated Magnesium Hip Stents, *J. Mater. Sci. Technol.*, 2021, **63**, p 145–160
41. T. Olugbade and J. Lu, Enhanced Corrosion Properties of Nanostructured 316 Stainless Steel in 0.6 M NaCl Solution, *J. Bio Tribo-Corros.*, 2019, **5**, p 38
42. T.O. Olugbade, Electrochemical Characterization of the Corrosion of Mild Steel in Saline Following Mechanical Deformation, *Anal. Lett.*, 2021, **54**, p 1055–1067
43. T. Olugbade, J. Lu, Improving the Passivity and Corrosion Behaviour of Mechanically Surface-Treated 301 Stainless Steel. In *International Conference on Nanostructured Materials (NANO 2020)*, 117, Australia (2020)
44. T. Olugbade, Datasets on the Corrosion Behaviour of Nanostructured AISI 316 Stainless Steel Treated by SMAT, *Data-in-brief*, 2019, **25**, p 104033
45. T.O. Olugbade and J. Lu, Characterization of the Corrosion of Nanostructured 17–4 PH Stainless Steel by Surface Mechanical Attrition Treatment (SMAT), *Anal. Lett.*, 2019, **52**, p 2454–2471
46. T. Olugbade, C. Liu and J. Lu, Enhanced Passivation Layer by Cr Diffusion of 301 Stainless Steel Facilitated by SMAT, *Adv. Eng. Mater.*, 2019, **21**, p 1900125
47. T.O. Olugbade and J. Lu, Literature Review on the Mechanical Properties of Materials After Surface Mechanical Attrition Treatment (SMAT), Nano, *Mater. Sci.*, 2020, **2**, p 3–31
48. K. Martin and F. Gerrit, Wrank W, Corrosion Fatigue Assessment of Creep-Resistant Magnesium Alloys DieMag422 and AE42, *Eng. Fract. Mech.*, 2017, **185**, p 33–45
49. A.K. Sabrina, BMd. Shahnewaz, M. Yukio, M. Yoshiharu and K. Toshikatsu, Corrosion Fatigue Behavior of Die-Cast and Shot-Blasted AM60 Magnesium Alloy, *Mater. Sci. Eng. A.*, 2011, **528**, p 1961–1966
50. H. Xiu-li, W. Ying-hui, H. Li-feng, Y. Zhi-feng, G. Chun-li and H. Peng-ju, Corrosion Fatigue Behavior of Epoxy-Coated Mg-3Al-1Zn Alloy in Gear Oil, *Trans. Nonferrous Met. Soc. China.*, 2014, **2014**(24), p 3429–3440
51. B.M. Shahnewaz and M. Yoshiharu, Corrosion Fatigue Behavior of Conversion Coated and Painted AZ61 Magnesium Alloy, *Int. J. Fatigue.*, 2011, **33**, p 1548–1556
52. BMd. Shahnewaz, M. Yoshiharu, M. Tsutomu and I. Shinpei, Corrosion Fatigue Behavior of Extruded Magnesium Alloy AZ61 Under Three Different Corrosive Environments, *Int. J. Fatigue*, 2008, **30**, p 1756–1765
53. X.N. Gu, W.R. Zhou, Y.F. Zheng, Y. Cheng, S.C. Wei, S.P. Zhong, T.F. Xi and L.J. Chen, Corrosion Fatigue Behaviors of Two Biomedical Mg Alloys—AZ91D and WE43—In Simulated Body fluid, *Acta Biomater.*, 2010, **6**, p 4605–4613
54. P. Wittke, M. Klein, F. Walther, Corrosion Fatigue Behaviour of Creep-Resistant Magnesium Alloy Mg-4Al-2Ba-2Ca. In *XVII International Colloquium on Mechanical Fatigue of Metals (ICMFM17)*, Procedia Eng. vol. 74, pp. 78–83 (2014)
55. R.R.K. Singh, J. Sajjad and E.H. Shervin, Corrosion Fatigue Fracture of Magnesium Alloys in Bioimplant Applications: A Review, *Eng. Fract. Mech.*, 2015, **137**, p 97–108
56. J. Sajjad, R.R.K. Singh, H. Chris and J. Davies, Corrosion Fatigue of a Magnesium Alloy in Modified Simulated Body fluid, *Eng. Fract. Mech.*, 2015, **137**, p 2–11
57. E.H. Shervin and R.R.K. Singh, Corrosion Fatigue of a Magnesium Alloy Under Appropriate Human Physiological Conditions for Bio-Implant Applications, *Eng. Fract. Mech.*, 2017, **186**, p 134–142
58. A.A. Renato and C.L.O. Mara, Corrosion Fatigue of Biomedical Metallic Alloys: Mechanisms and Mitigation, *Acta Biomater.*, 2012, **8**, p 937–962
59. X.L. He, Y.H. Wei, L.F. Hou, Z.F. Yan, C.L. Guo and P.J. Han, Investigation on Corrosion Fatigue Property of Epoxy Coated AZ31

Magnesium Alloy in Sodium Sulfate Solution, *Theor. Appl. Fract. Mech.*, 2014, **70**, p 39–48
60. S. Ishihara, K. Masud, T. Namito, S. Sunada and H. Notoya, On Corrosion Fatigue Strength of the Anodized and Painted Mg Alloy, *Int. J. Fatigue.*, 2014, **66**, p 252–258
61. J. Sajjad, R.K. Singh, H.J. Chris, J. Davies, J.J. Hofstetter, J. Peter, J. Uggowitzer and F.L. Jörg, Stress Corrosion Cracking and Corrosion Fatigue Characterisation of MgZn1Ca0.3 (ZX10) in a Simulated Physiological Environment, *J. Mech. Behav. Biomed. Mater.*, 2017, **65**, p 634–643
62. S. Ishihara, T. Namito, H. Notoya and A. Okada, The Corrosion Fatigue Resistance of an Electrolytically-Plated Magnesium Alloy, *Int. J. Fatigue.*, 2010, **32**, p 1299–1305
63. S. Jalota, S.B. Bhaduri and A.C. Tas, Using a Synthetic Body Fluid (SBF) Solution of 27 mM HCO_3− to Make Bone Substitutes More Osteointegrative, *Mater. Sci. Eng. C*, 2008, **28**, p 129–140
64. A. Oyane, H.-M. Kim, T. Furuya, T. Kokubo, T. Miyazaki and T. Nakamura, Preparation and Assessment of Revised Simulated Body Fluids, *J. Biomed. Mater. Res.*, 2003, **65A**, p 188–195
65. A. Yamamoto and S. Hiromoto, Effect of Inorganic Salts, Amino Acids and Proteins on the Degradation of Pure Magnesium In Vitro, *Mater. Sci. Eng. C.*, 2009, **29**, p 1559–1568
66. Y. Xin, T. Hu and P.K. Chu, Influence of Test Solutions on In Vitro Studies of Biomedical Magnesium Alloys, *J. Electrochem. Soc.*, 2010, **157**, p C238–C243
67. T. Kokubo and H. Takadama, How Useful is SBF in Predicting in vivo Bone Bioactivity?, *Biomaterials*, 2006, **27**, p 2907–2915
68. Y. Xin, T. Hu and P.K. Chu, In Vitro Studies of Biomedical Magnesium Alloys in a Simulated Physiological Environment: A Review, *Acta Biomater.*, 2011, **7**, p 1452–1459
69. L. Yang, H. Hort, R. Willumeit and F. Feyerabend, Effects of Corrosion Environment and Proteins on Magnesium Corrosion, *Corros. Eng. Sci. Technol.*, 2012, **47**, p 335–339
70. J. Hofstetter, M. Becker, E. Martinelli, A.M. Weinberg, B. Mingler, H. Kilian et al., High-Strength Low-Alloy (HSLA) Mg-Zn-Ca Alloys with Excellent Biodegradation Performance, *JOM.*, 2014, **66**, p 566–572
71. R. Rettig and S. Virtanen, Time-Dependent Electrochemical Characterization of the Corrosion of a Magnesium Rare-Earth Alloy in Simulated Body Fluids, *J. Biomed. Mater. Res. A.*, 2008, **85A**, p 167–175
72. P. Jiang, C. Blawert, J. Bohlen and M.L. Zheludkevich, Corrosion Performance, Corrosion Fatigue Behavior and Mechanical Integrity of an Extruded Mg4Zn0.2Sn Alloy, *J. Mater. Sci. Technol.*, 2020, **59**, p 107–116
73. P. Jiang, C. Blawert, R. Hou, J. Bohlen, N. Konchakova and M.L. Zheludkevich, A Comprehensive Comparison of the Corrosion Performance, Fatigue Behavior and Mechanical Properties of Micro-alloyed MgZnCa and MgZnGe Alloys, *Mater. Des.*, 2020, **185**, p 108285
74. M. Liu, J. Wang, S. Zhu, Y. Zhang, Y. Sun, L. Wang and S. Guan, Corrosion Fatigue of the Extruded Mg-Zn-Y-Nd Alloy in Simulated Body Fluid, *J. Magnes. Alloys.*, 2020, **8**, p 231–240
75. A. Maldar, L. Wang, G. Zhu and X. Zeng, Investigation of the Alloying Effect on Deformation Behavior in Mg by Visco-Plastic Self-Consistent Modeling, *J. Magnes. Alloys.*, 2020, **8**, p 210–218
76. V.K. Bommala, M.G. Krishna and C.T. Rao, Magnesium Matrix Composites for Biomedical Applications: A Review, *J. Magnes. Alloys.*, 2019, **7**, p 72–79
77. N. Sezer, Z. Evis and S.M. Kayhan, Review of Magnesium-Based Biomaterials and Their Applications, *J. Magnes. Alloys.*, 2018, **6**, p 23–43
78. W.Y. Jiang, J.F. Wang, W.K. Zhao, Q.S. Liu, D.M. Jiang and S.F. Guo, Effect of Sn Addition on the Mechanical Properties and Bio-Corrosion Behavior of Cytocompatible Mg-4Zn Based Alloys, *J. Magnes. Alloys.*, 2019, **7**, p 15–26
79. Y. Liu, Y.F. Zheng, X.H. Chen, J.A. Yang, H.B. Pan, D.F. Chen, L.N. Wang, J.L. Zhang, D.H. Zhu, S.L. Wu, K.W.K. Yeung, R.C. Zeng, Y. Han and S.K. Guan, Fundamental Theory of Biodegradable Metals—Definition, Criteria, and Design, *Adv. Funct. Mater.*, 2019, **29**, p 1–21
80. Y. Li, Y. Zhou, Z.M. Shi, J. Venezuela, A. Soltan and A. Atrens, Stress Corrosion Cracking of EV31A in 0.1 M Na2SO4 Saturated with Mg(OH)2, *J. Magnes. Alloys.*, 2018, **6**, p 337–345
81. M. Sabbaghian, R. Mahmudi and K.S. Shin, Effect of Texture and Twinning on Mechanical Properties and Corrosion Behavior of an Extruded Biodegradable Mg-4Zn Alloy, *J. Magnes. Alloys.*, 2019, **7**, p 707–716
82. W.B. Du, K. Liu, K. Ma, Z.H. Wang and S.B. Li, Effects of Trace Ca/Sn Addition on Corrosion Behaviors of Biodegradable Mg-4Zn-0.2Mn Alloy, *J. Magnes. Alloys.*, 2018, **6**, p 1–14
83. S. Jafari, S.E. Harandi and R.K. Singh Raman, A Review of Stress-Corrosion Cracking and Corrosion Fatigue of Magnesium Alloys for Biodegradable Implant Applications, *JOM.*, 2015, **67**, p 1143–1153
84. R. Bonan and A.W. Asgar, Biodegradable Stents—Where Are We in 2009?, *US Cardiol.*, 2009, **6**, p 81–84
85. Y.F. Zheng, X.N. Gu, Y.L. Xi and D.L. Chai, In Vitro Degradation and Cytotoxicity of Mg/Ca Composites Produced by Powder Metallurgy, *Acta Biomater.*, 2010, **6**, p 1783–1791
86. T. Pollock, Weight Loss with Magnesium Alloys, *Science*, 2010, **328**, p 986–987
87. M. Razavi, M.H. Fathi and M. Meratian, Microstructure, Mechanical Properties and Bio-Corrosion Evaluation of Biodegradable AZ91-FA Nanocomposites for Biomedical Applications, *Mater. Sci. Eng. A*, 2010, **527**, p 6938–6944
88. S. Cai, F. Feng, N. Li, T. Lei and W. Tang, On the Corrosion Behaviour of Newly Developed Biodegradable Mg-Based Metal Matrix Composites Produced by In Situ Reaction, *Corros. Sci.*, 2012, **54**, p 270–277
89. G. Manivasagam and S. Suwas, Biodegradable Mg and Mg Based Alloys for Biomedical Implants, *Mater. Sci. Technol. Lond.*, 2014, **30**, p 515–520
90. H. Li, Q.M. Peng, X.J. Li, K. Li, Z.S. Han and D.Q. Fang, A New Sand-Wedge-Forming Mechanism in an Extra-Arid Area, *Mater. Des.*, 2014, **58**, p 43–51
91. N. Hort, Y. Huang, D. Fechner, M. Stormer, C. Blawert, F. Witte, C. Vogt, H. Drucker, R. Willumeit, K.U. Kainer and F. Feyerabend, Magnesium Alloys as Implant Materials—Principles of Property Design for Mg-RE Alloys, *Acta Biomater.*, 2010, **6**, p 1714–1725
92. X.N. Gu, Y.F. Zheng, S.P. Zhong, T.F. Xi, J.Q. Wang and W.H. Wang, Corrosion of, and Cellular Responses to Mg-Zn-Ca Bulk Metallic Glasses, *Biomaterials*, 2010, **31**, p 1093–1103
93. Y. Cheng, S.P. Zhong, X.N. Gu, Y.F. Zheng and T.F. Xi, Study of Oxidation-Reduction Potential (ORP) on Autothermal Thermophilic Aerobic Digestion Process, *Biomaterials*, 2009, **30**, p 484–498
94. S. Dumoulin, P.C. Skaret, H.J. Roven, Y.J. Chen, Y.J. Li and J.C. Walmsley, Microstructure Evolution of Commercial Pure Titanium During Equal Channel Angular Pressing, *Mater. Sci. Eng. A Struct. Mater.*, 2010, **527**, p 789–796
95. T. Shibata, Y. Nakamura, Y. Tsumura, Y. Tonogai and Y. Ito, Differences in Behavior Among the Chlorides of Seven Rare Earth Elements Administered Intravenously to Rats, *Fundam. Appl. Toxicol.*, 1997, **37**, p 106–116
96. G.J. Dias, M.P. Staiger, N.T. Kirkland, I. Kolbeinsson and T. Woodfield, *Mater. Lett.*, 2010, **64**, p 2572–2574
97. G.J. Dias, M.P. Staiger, N.T. Kirkland, I. Kolbeinsson and T. Woodfield, *Int. J. Mod. Phys. B.*, 2009, **23**, p 1002–1008
98. N. Kuromoto, R. Simao and G. Soares, *J. Mater. Charact.*, 2007, **58**, p 114–121
99. K.H. Rashid, A.A. Khadom and H.B. Mahood, Aluminum ASA 6061 Anodizing Process by Chromic Acid Using Box–Wilson Central Composite Design: Optimization and Corrosion Tendency, *Met. Mater. Int.*, 2020 https://doi.org/10.1007/s12540-020-00762-1
100. S.A. Ajeel and U.S. Mohammad, The Determination of Optimum Conditions for Anodizing Aluminum Alloy (6063), *Eng. Technol.*, 2008, **26**, p 1341–1354
101. Q. Xu, A. Ma, Y. Li, J. Sun, Y. Yuan, J. Jiang and C. Ni, Microstructure Evolution of AZ91 Alloy Processed by a Combination Method of Equal Channel Angular Pressing and Rolling, *J. Magnes. Alloys.*, 2020, **8**, p 192–198
102. G.E. Thompson, The Effect of Current Density on Anodic Film Growth on Al-Cu Alloy. In *Proceeding of 2nd International Symposium on Aluminum Surface Science and Technology, Manchester*, pp. 21–186, (2000)
103. M.M. Rahman, E. Garcia-Caurel, A. Santos, L. Marsal, J. Pallarès and J. Ferré-Borrull, Effect of the Anodization Voltage on the Pore-Widening Rate of Nanoporous Anodic Alumina, *Nanoscale Res. Lett.*, 2012, **7**, p 474

104. Y. Huang, H. Zeng, C. Zhao, Y. Qu and P. Zhang, Kinetic Models of Controllable Pore Growth of Anodic Aluminum Oxide Membrane, *Met. Mater. Int.*, 2012, **18**, p 433–438
105. M.M. Jalilvand, M. Akbarifar, M. Divandari and H. Saghafian, On the Dynamically Formed Oxide Films in Molten Mg, *J. Magnes. Alloys.*, 2020, **8**, p 219–230
106. M. Roshani, A.S. Rouhaghdam, M. Aliofkhazraei and A.H. Astaraee, Optimization of Mechanical Properties for Pulsed Anodizing of Aluminum: The Effect of Electrolyte and Temperature, *Surf. Coat. Technol.*, 2017, **310**, p 17–24
107. W. Bensalah, M. DePetris-Wery and H.F. Ayedi, Young's Modulus of Anodic Oxide Layers Formed on Aluminum in Sulphuric Acid Bath, *Mater. Lett.*, 2016, **179**, p 82–85
108. W.J. Stepniowski and Z. Bojar, Synthesis of Anodic Aluminum Oxide (AAO) at Relatively High Temperatures. Study of the Influence of Anodization Conditions on the Alumina Structural Features, *Surf. Coat. Technol.*, 2011, **206**, p 256–272
109. Y. Zhang and T. Lin, Influence of Duty Cycle on Properties of the Superhydrophobic Coating on an Anodized Magnesium Alloy Fabricated by Pulse Electrodeposition, *Colloids Surf. A.*, 2019, **568**, p 43–50
110. J. Han, C. Blawert, S. Tang, J. Yang, J. Hu and M. Zheludkevich, Effect of Surface Pre-Treatments on the Formation and Degradation Behaviour of a Calcium Phosphate Coating on Pure Magnesium, *Coatings*, 2019, **9**, p 259
111. N. Aboudzadeh, C. Dehghanian and M. Shokrgozar, Effect of Electrodeposition Parameters and Substrate on Morphology of Si-HA Coating, *Surf. Coat. Technol.*, 2019, **375**, p 341–351
112. W. Wu, Z. Wang, S. Zang, X. Yu, H. Yang and S. Chang, Research Progress on Surface Treatments of Biodegradable Mg Alloys: A Review, *ACS Omega*, 2020, **5**, p 941–947
113. J. Syu, J. Uan, M. Lin and Z. Lin, Optically Transparent Li-Al-CO_3 Layered Double Hydroxide Thin Films on an AZ31 Mg Alloy Formed by Electrochemical Deposition and Their Corrosion Resistance in a Dilute Chloride Environment, *Corros. Sci.*, 2013, **68**, p 238–248
114. H. Bakhsheshi-Rad, A. Ismail, M. Aziz, Z. Hadisi, M. Omidi and X. Chen, Antibacterial Activity and Corrosion Resistance of Ta_2O_5 Thin Film and Electrospun PCL/MgO-Ag Nanofiber Coatings on Biodegradable Mg Alloy Implants, *Ceram. Int.*, 2019, **45**, p 11883–11892
115. T.O. Olugbade, Stress Corrosion Cracking and Precipitation Strengthening Mechanism in TWIP Steels: Progress and Prospects, *Corros. Rev.*, 2020, **38**, p 473–488
116. W. Xia, N. Li, B. Deng, R. Zheng and Y. Chen, Corrosion Behavior of a sol-gel ZrO_2 Pore-Sealing Film Prepared on a Microarc Oxidized Aluminum Alloy, *Ceram. Int.*, 2019, **45**, p 11062–11067
117. Y. Castro and A. Duran, Control of Degradation Rate of Mg Alloys Using Silica Sol−Gel Coatings for Biodegradable Implant Materials, *J. Sol-Gel Sci. Technol.*, 2019, **90**, p 198–208
118. M. Park, J. Lee, C. Park, S. Lee, H. Seok and Y. Choy, Polycaprolactone coating with varying thicknesses for controlled corrosion of magnesium, *J. Coat. Technol. Res.*, 2013, **10**, p 695–706
119. Z. Hu, J. Zhang, S. Xiong and Y. Zhao, Performance of Polymer Solar Cells Fabricated by Dip Coating Process, *Sol. Energy Mater. Sol. Cells.*, 2012, **99**, p 221–225
120. R.O. Hussein, D.O. Northwood and X. Nie, The Effect of Processing Parameters and Substrate Composition on the Corrosion Resistance of Plasma Electrolytic Oxidation (PEO) Coated Magnesium Alloys, *Surf. Coat. Technol.*, 2013, **237**, p 357–368
121. L. Zhang, J. Zhang, C. Chen and Y. Gu, Advances in Microarc Oxidation Coated AZ31 Mg Alloys for Biomedical Applications, *Corros. Sci.*, 2015, **91**, p 7–28
122. M. Dziaduszewska, M. Shimabukuro, T. Seramak, A. Zielinski and T. Hanawa, Effects of Micro-Arc Oxidation Process Parameters on Characteristics of Calcium-Phosphate Containing Oxide Layers on the Selective Laser Melted Ti13Zr13Nb Alloy, *Coatings*, 2020, **10**, p 745
123. L.C. Zhang, L.Y. Chen and L. Wang, Surface Modification of Titanium and Titanium Alloys: Technologies, Developments, and Future Interests, *Adv. Eng. Mater.*, 2020, **22**, p 1901258
124. X.J. Tao, S.J. Li, C.Y. Zheng, J. Fu, Z. Guo, Y.L. Hao, R. Yang and Z.X. Guo, Synthesis of a Porous Oxide Layer on a Multifunctional Biomedical Titanium by Micro-arc Oxidation, *Mater. Sci. Eng. C.*, 2009, **29**, p 1923–1934
125. S.A. Alves, R. Bayón, V.S. de Viteri, M.P. Garcia, A. Igartua, M.H. Fernandes and L.A. Rocha, Tribocorrosion Behavior of Calcium- and Phosphorous-Enriched Titanium Oxide Films and Study of Osteoblast Interactions for Dental Implants, *J. Bio- Tribo-Corros.*, 2015, **1**, p 1–21
126. L. Zaraska, K. Gawlak, M. Gurgul, D. Gilek, M. Kozieł, R.P. Socha and G.D. Sulka, Morphology of Nanoporous Anodic Films Formed on Tin During Anodic Oxidation in Less Commonly Used Acidic and Alkaline Electrolytes, *Surf. Coat. Technol.*, 2019, **362**, p 191–199
127. T. Liu, Q. Yang, N. Guo, Y. Lu and B. Song, Stability of Twins in Mg Alloys—A Short Review, *J. Magnes. Alloys.*, 2020, **8**, p 66–77
128. W. Mu and Y. Han, Characterization and Properties of the MgF_2/ZrO $_2$ Composite Coatings on Magnesium Prepared by Micro-arc Oxidation, *Surf Coat Technol.*, 2008, **202**, p 4278–4284
129. Y. Gu, S. Bandopadhyay, C.F. Chen, Y. Guo and C. Ning, Effect of Oxidation Time on the Corrosion Behavior of Micro-arc Oxidation Produced AZ31 Magnesium Alloys in Simulated Body Fluid, *J. Alloys Compd.*, 2012, **543**, p 109–117
130. Y. Tang, X. Zhao, K. Jiang, J. Chen and Y. Zuo, The Influences of Duty Cycle on the Bonding Strength of AZ31B Magnesium Alloy by Microarc Oxidation Treatment, *Surf. Coat. Technol.*, 2010, **205**, p 1789–1792
131. I.J. Hwang, Y.G. Ko, K.M. Lee and D.H. Shin, Effect of Pulse Frequency on Corrosion Behavior of AZ91 Mg Alloy Treated by Microarc Discharge Oxidation Coating, *Mater. Trans.*, 2011, **52**, p 580–583
132. Y. Gu, C.F. Chen, S. Bandopadhyay, C. Ning, Y. Zhang and Y. Guo, Corrosion Mechanism and Model of Pulsed DC Microarc Oxidation Treated AZ31 Alloy in Simulated Body Fluid, *Appl. Surf. Sci.*, 2012, **258**, p 6116–6126
133. Y. Han, S.H. Hong and K. Xu, Structure and In Vitro Bioactivity of Titania-Based Films by Micro-Arc Oxidation, *Surf. Coat. Technol.*, 2003, **168**, p 249–258
134. Z. Zhang, G. Wu, A. Atrens and W. Ding, Influence of Trace As Content on the Microstructure and Corrosion Behavior of the AZ91 Alloy in Different Metallurgical Conditions, *J. Magnes. Alloys.*, 2020, **8**, p 301–317
135. J.M. Li, Q.W. Zhang, H. Cai, A.J. Wang, J.M. Zhang and X.H. Hua, Controlled Deposition, Electrical and Electrochemical Properties of Electroless Nickel Layers on Microarc Oxidized Magnesium Substrates, *Mater. Lett.*, 2013, **93**, p 263–265
136. H.F. Guo, M.Z. An, H.B. Huo, S. Xu and L.J. Wu, Microstructure Characteristic of Ceramic Coatings Fabricated on Magnesium Alloys by Micro-arc Oxidation in Alkaline Silicate Solutions, *Appl. Surf. Sci.*, 2006, **252**, p 7911–7916
137. X.G. Han, X.P. Zhu and M.K. Lei, Electrochemical Properties of Microarc Oxidation Films on a Magnesium Alloy Modified by High-Intensity Pulsed Ion Beam, *Surf. Coat. Technol.*, 2011, **206**, p 874–878
138. A. Seyfoori, S. Mirdamadi, A. Khavandi and Z.S. Raufi, Biodegradation Behavior of Micro-arc Oxidized AZ31 Magnesium Alloys Formed in Two Different Electrolytes, *Appl. Surf. Sci.*, 2012, **261**, p 92–100
139. M. Karl and J.R. Kelly, Influence of Loading Frequency on Implant Failure Under Cyclic Fatigue Conditions, *Dent. Mater.*, 2009, **25**, p 1426–1432
140. P.B. Srinivasan, J. Liang, C. Blawert and W. Dietzel, Environmentally Assisted Cracking Behaviour of Plasma Electrolytic Oxidation Coated AZ31 Magnesium Alloy, *Corros. Eng. Sci. Technol.*, 2011, **46**, p 706–711
141. Z. Shi, M. Liu and A. Atrens, Measurement of the Corrosion Rate of Magnesium Alloys Using Tafel Extrapolation, *Corros. Sci.*, 2010, **52**, p 579–588
142. W.B. Xue, Z.W. Deng, R.Y. Chen and T.H. Zhang, Growth Regularity of Ceramic Coatings Formed by Microarc Oxidation on Al-Cu-Mg Alloy, *Thin Solid Films*, 2000, **372**, p 114–117
143. G. Sundararajan and L.R. Krishna, Mechanisms Underlying the Formation of Thick Alumina Coatings Through the MAO Coating Technology, *Surf. Coat. Technol.*, 2003, **167**, p 269–277
144. R. Arrabal, J.M. Mota, A. Criado, A. Pardo, M. Mohedano and E. Matykina, Assessment of Duplex Coating Combining Plasma Electrolytic Oxidation and Polymer Layer on AZ31 Magnesium Alloy, *Surf. Coat. Technol.*, 2012, **206**, p 4692–4703

145. W. Yang, P. Wang, Y.C. Guo, B.L. Jiang, F. Yang and J.P. Li, Microstructure and Corrosion Resistance of Modified AZ31 Magnesium Alloy Using Microarc Oxidation Combined with Electrophoresis Process, *J. Wuhan Univ. Technol.*, 2013, **28**, p 612–616
146. Y.H. Gu, W.M. Xiong, C.Y. Ning and J. Zhang, Residual Stresses in Microarc Oxidation Ceramic Coatings on Biocompatible AZ31 Magnesium Alloys, *J. Mater. Eng. Perform.*, 2012, **21**, p 1085–1090
147. D.E. Packham, Surface Energy, Surface Topography and Adhesion, *Int. J. Adhes. Adhes.*, 2003, **23**, p 437–448
148. G.W. Critchlow and D.M. Brewis, Review of Surface Pretreatments for Aluminium Alloys, *Int. J. Adhes. Adhes.*, 1996, **16**, p 255–275
149. G.W. Critchlow, K.A. Yendall, D. Bahrani, A. Quinn and F. Andrews, Strategies for the Replacement of Chromic Acid Anodising for the Structural Bonding of Aluminium Alloys, *Int. J. Adhes. Adhes.*, 2006, **26**, p 419–453
150. C. Zhao, F. Cao and G. Song, Corrosivity of Haze Constituents to Pure Mg, *J. Magnes. Alloys.*, 2020, **8**, p 150–162
151. I.B. Singh, M. Singh and S. Das, A Comparative Corrosion Behavior of Mg, AZ31 and AZ91 Alloys in 3.5% NaCl Solution, *J. Magnes. Alloys.*, 2015, **3**, p 142–148
152. B.R. Sunil, C. Ganapathy, T.S. Sampath and K.U. Chakkingal, Processing and Mechanical Behavior of Lamellar Structured Degradable Magnesium-Hydroxyapatite Implants, *J. Mech. Behav. Biomed. Mater.*, 2014, **40**, p 178–189
153. X. Gu, Y. Zheng, Y. Cheng, S. Zhong and T. Xi, In Vitro Corrosion and Biocompatibility of Binary Magnesium Alloys, *Biomaterials*, 2009, **30**, p 484–498
154. X.N. Gu, X.H. Xie, N. Li, Y.F. Zheng and L. Qin, In Vitro and In Vivo Studies on a Mg-Sr Binary Alloy System Developed as a New Kind of Biodegradable Metal, *Act. Biomater.*, 2012, **8**, p 2360–2374
155. Z. Li, X. Gu, S. Lou and Y. Zheng, The Development of Binary Mg-Ca Alloys for Use as Biodegradable Materials Within Bone, *Biomaterials*, 2008, **29**, p 1329–1344
156. G. Song, A.L. Bowles and D.H. StJohn, Corrosion Resistance of Aged Die Cast Magnesium Alloy AZ91D, *Mater. Sci. Eng. A.*, 2004, **366**, p 74–86
157. F. Witte, V. Kaese, H. Haferkamp, E. Switzer, A. Meyer-Lindenberg, C.J. Wirth and H. Windhagen, In Vivo Corrosion of Magnesium Alloys and the Associated Bone Response, *Biomaterials*, 2005, **26**, p 3557–3563
158. P. Minárik, R. Král, J. Pešička and F. Chmelík, Evolution of Mechanical Properties of LAE442 Magnesium Alloy Processed by Extrusion and ECAP, *J. Mater. Res. Technol.*, 2015, **4**, p 75–78
159. A. Bahmani, S. Arthanari and K.S. Shin, Improved Corrosion Resistant and Strength of a Magnesium Alloy Using Multi-directional Forging (MDF), *Int. J. Adv. Manuf. Technol.*, 2019, **105**, p 785–797
160. L.B. Tong, Q.X. Zhang, Z.H. Jiang, J.B. Zhang, J. Meng, L.R. Cheng and H.J. Zhang, Microstructures, Mechanical Properties and Corrosion Resistances of Extruded Mg-Zn-Ca-*x*Ce/La Alloys, *J. Mech. Behav. Biomed. Mater.*, 2016, **62**, p 57–70
161. F. Cao, Z. Shi, G.L. Song, M. Liu and A. Atrens, Corrosion Behaviour in Salt Spray and in 3.5% NaCl Solution Saturated with Mg(OH)2 of As-Cast and Solution Heat-Treated Binary Mg-X Alloys: X=Mn, Sn, Ca, Zn, Al, Zr, Si, Sr, *Corros Sci.*, 2013, **76**, p 60–97
162. F. Cao, Z. Shi, G.L. Song, M. Liu, M.S. Dargusch and A. Atrens, Influence of Hot Rolling on the Corrosion Behavior of Several Mg-X Alloys, *Corros Sci.*, 2015, **90**, p 176–191
163. Z. Shi, F. Cao, G.L. Song, M. Liu and A. Atrens, Corrosion Behaviour in Salt Spray and in 3.5% NaCl Solution Saturated with Mg(OH)2 of As-Cast and Solution Heat-Treated Binary Mg-RE Alloys: RE=Ce, La, Nd, Y, Gd, *Corros Sci.*, 2013, **76**, p 98–118
164. G. Bi, Y. Li, S. Zang, J. Zhang, Y. Ma and Y. Hao, Microstructure, Mechanical and Corrosion Properties of Mg-2Dy-xZn (x=0, 0.1, 0.5 and 1 at.%) Alloys, *J. Magnes. Alloys*, 2014, **2**, p 64–71
165. J. Hu, Q. Li and H. Gao, Influence of Twinning Texture on the Corrosion Fatigue Behavior of Extruded Magnesium Alloys, *Acta Metall. Sin. (Engl. Lett.)*, 2021, **34**, p 65–76
166. A. Bahmani, S. Arthanari and K.S. Shin, Formulation of Corrosion Rate of Magnesium Alloys Using Microstructural Parameters, *J. Magnes. Alloys*, 2020, **8**(2020), p 134–149
167. R. Xin, Y. Luo, A. Zuo, J. Gao and Q. Liu, Texture Effect on Corrosion Behavior of AZ31 Mg Alloy in Simulated Physiological Environment, *Mater. Lett.*, 2012, **72**, p 1–4
168. G.L. Song, R. Mishra and Z. Xu, Crystallographic Orientation and Electrochemical Activity of AZ31 Mg Alloy, *Electrochem. Commun.*, 2010, **12**, p 1009–1012
169. G.L. Song, The Effect of Texture on the Corrosion Behavior of AZ31 Mg Alloy, *JOM*, 2012, **64**, p 671–679
170. S. Bahl, S. Suwas and K. Chatterjee, The Control of Crystallographic Texture in the Use of Magnesium as a Resorbable Biomaterial, *RSC Adv.*, 2014, **4**, p 55677–55684
171. Z. Pu, G.L. Song, S. Yang, J.C. Outeiro, O.W. Dillon, D.A. Puleo and I.S. Jawahir, Grain Refined and Basal Textured Surface Produced by Burnishing for Improved Corrosion Performance of AZ31B Mg Alloy, *Corros. Sci.*, 2012, **57**, p 192–201
172. E. Mostaed, M. Hashempour, A. Fabrizi, D. Dellasega, M. Bestetti, F. Bonollo and M. Vedani, Microstructure, Texture Evolution, Mechanical Properties and Corrosion Behavior of ECAP Processed ZK60 Magnesium Alloy for Biodegradable Applications, *J. Mech. Behav. Biomed. Mater.*, 2014, **37**, p 307–322
173. Z. Sajuri, Y. Miyashita, Y. Mutoh and Y. Hosokai, Effect of Texture on Fatigue Properties of an Extruded AZ61 Magnesium Alloy Plate, *Key Eng. Mater.*, 2004, **274–276**, p 193–198
174. X. Ying, Y. Zengyuan, Z. Tao and J. Yanyao, Effect of Texture Evolution on Corrosion Resistance of AZ80 Magnesium Alloy Subjected to Applied Force in Simulated Body Fluid, *Mater. Res. Express*, 2020, **7**, p 015406